

Localized interfacial Phonon Modes at the Electronic Axion Domain Wall

Abhinava Chatterjee¹, Mourad Oudich², Yun Jing², and Chao-Xing Liu^{*1}

¹*Department of Physics, The Pennsylvania State University, University Park, Pennsylvania 16802, USA*

²*Graduate Program in Acoustics, The Pennsylvania State University, University Park, Pennsylvania 16802, USA*

(Dated: March 13, 2024)

The most salient feature of electronic topological states of matter is the existence of exotic electronic modes localized at the surface or interface of a sample. In this work, in an electronic topological system, we demonstrate the existence of localized phonon modes at the domain wall between topologically trivial and non-trivial regions, in addition to the localized interfacial electronic states. In particular, we consider a theoretical model for the Dirac semimetal with a gap opened by external strains and study the phonon dynamics, which couples to electronic degrees of freedom via strong electron-phonon interaction. By treating the phonon modes as a pseudo-gauge field, we find that the axion type of terms for phonon dynamics can emerge in gapped Dirac semimetal model and lead to interfacial phonon modes localized at the domain wall between trivial and non-trivial regimes that possess the axion parameters 0 and π , respectively. We also discuss the physical properties and possible experimental probe of such interfacial phonon modes.

Introduction - At the surface of a topological electronic material or at the domain wall between two topologically distinct regions, surface or interfacial electronic modes can emerge and exhibit exotic physical phenomena [1–4]. The existence of these surface/interfacial electronic modes is a direct consequence of non-trivial topology of the bulk electronic band structure in topological materials, a general feature summarized as the bulk–boundary correspondence [5–11]. The connection between bulk topological states and the corresponding boundary modes is not limited to electronic states, but has also been generalized to other physical systems, including photonics [12, 13], phononics [14–16], magnonics [17, 18], electric circuits [19, 20], and mechanical systems [21–23], in which a variety of boundary modes have been identified and classified, and many of them have been experimentally observed.

Our current understanding and classification of topological states and boundary modes (e.g. electrons, phonons, magnons, *etc.*) is mainly limited to systems with one type of quasi-particles. As the interaction between different quasi-particles, e.g. electron-phonon interaction, generally exists in realistic materials [24–29], one may ask if topological states and the boundary modes of different quasi-particles are connected to each other. Topological polariton [30–35] provides such an example. Here we wonder, in a system with strong electron-phonon interaction, if a boundary phonon mode can exist for a topologically non-trivial electronic system.

In this work, we give an affirmative answer to this question and show that an interfacial phonon mode can exist at the domain wall between two topologically distinct regions with different electronic axion parameters. Particularly, we consider the Dirac semimetal model with a small gap controlled by external static strain serving as effective axion fields. Acoustic phonon dynamics is strongly influenced by the axion term through electron-acoustic-phonon (or equivalently electron-strain) interaction, which gives rise to interfacial phonon modes localized at the domain wall between topologically trivial and

non-trivial regions of electronic states.

Electron-phonon Interaction and Valley Axion Field in Gapped Dirac Semimetals - We consider three-dimensional (3D) Dirac semimetal, e.g. Na₃Bi [36, 37], with electron-phonon coupling, described by the Hamiltonian $H = H_e + H_{e-ph}$. H_e is the model Hamiltonian for 3D Dirac semimetals [38, 39], and its detailed form is described in Sec.S1 B of Supplementary Materials (SM) [40]. The crystal symmetry of H_e is described by the D_{6h} group that can be generated by six-fold rotation \hat{C}_{6z} , inversion \hat{I} and two-fold rotation \hat{C}_{2x} . The conduction and valence bands of H_e have the crossings located at the momenta $\mathbf{K}_a = (0, 0, ak_c)$ with $a = \pm$ and k_c depending on material parameters. Around these crossing points, the effective Hamiltonians behave as 3D massless Dirac fermions with nodes protected by \hat{C}_{6z} , as schematically depicted in Fig. 1(a)(i). The index $a = \pm$ in \mathbf{K}_a is regarded as two "valleys" that are related by time reversal \hat{T} . For electron-phonon interaction, we consider acoustic phonons that can be described by the strain tensor $u_{ij} = \frac{1}{2}(\partial_i u_j + \partial_j u_i)$ ($i, j = x, y, z$) with \mathbf{u} labelling the displacement field [41]. Based on the D_{6h} group for Na₃Bi, we can construct all the terms up to the linear orders in both the momentum \mathbf{k} and strain tensor u_{ij} (See Sec.S1 B of SM) [40].

We next project the total Hamiltonian H into the subspace spanned by the massless Dirac fermions at \mathbf{K}_a , and the corresponding effective Hamiltonian is written as $H_{eff} = \sum_{a=\pm} H_{eff,a}$ with $H_{eff,a}$ given by

$$H_{eff,a} = A_0^{pse} \mathbb{I} + A_0 \pi_x \Gamma_3 - A_0 \pi_y \Gamma_4 - 2M_1 k_c \pi_z \Gamma_5 + |m| (\cos \Phi_a \Gamma_1 - \sin \Phi_a \Gamma_2), \quad (1)$$

where $\boldsymbol{\pi} = \mathbf{k} - \mathbf{A}_a^{pse}$ with the pseudo-gauge field [42–45] $A_0^{pse} = \tilde{C}(\{u_{ij}\})$ and $\mathbf{A}_a^{pse} = a [-A_4 k_c u_{xz}, A_4 k_c u_{yz}, \tilde{M}(\{u_{ij}\})]$ ($a = \pm$). Here $\tilde{C}(\{u_{ij}\}) = C_3 u_{zz} + C_4 (u_{xx} + u_{yy})$, $\tilde{M}(\{u_{ij}\}) = M_3 u_{zz} + M_4 (u_{xx} + u_{yy})$, $|m| = Dk_c \sqrt{(2u_{xy})^2 + (u_{xx} - u_{yy})^2}$,

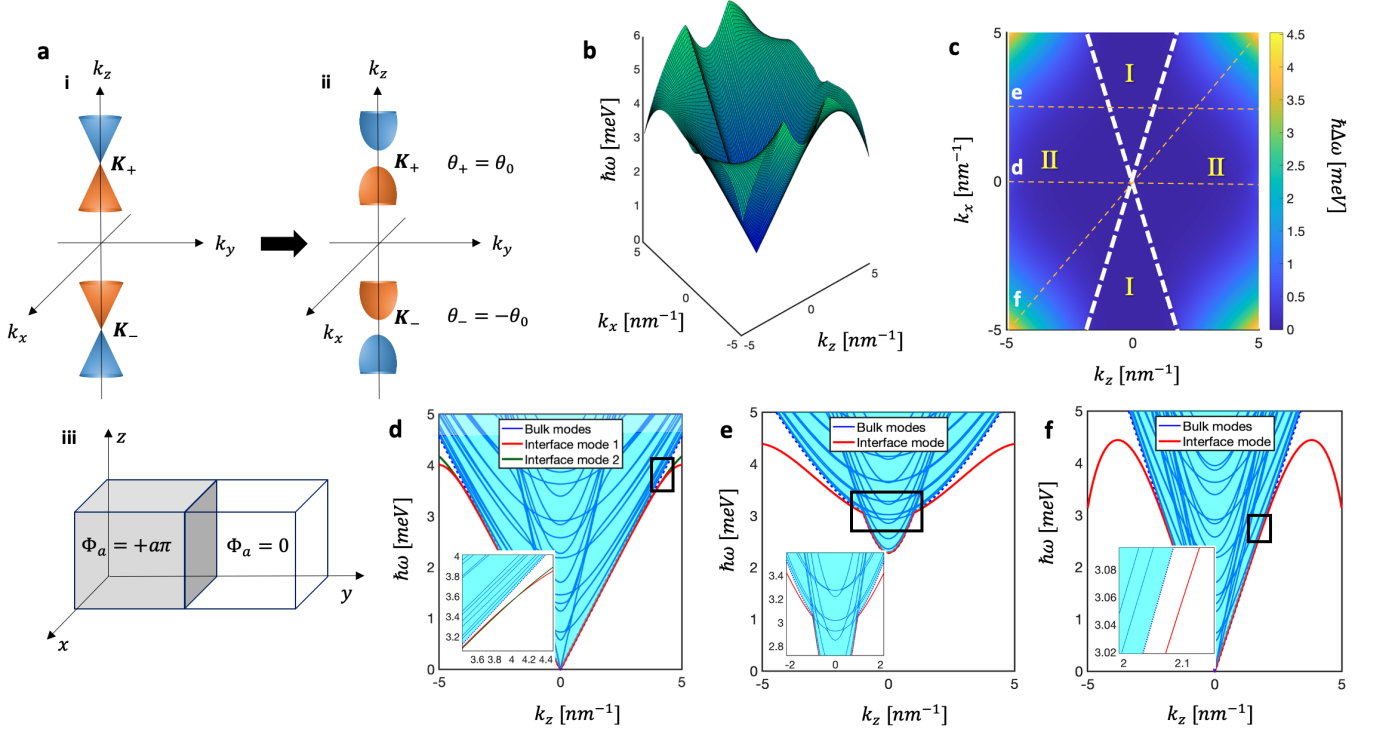


FIG. 1. (a) Setup. (i) The spectrum for Na_3Bi is gapless at the K_{\pm} points. (ii) The external strain leads to a gap in the spectrum where $\theta_0 = \pi/2$ by choosing the static strain $u_{xy}^0 \rightarrow 0$ and $u_{xx}^0 - u_{yy}^0 \neq 0$. (iii) The variation of the static axion angle along the y direction which induces a domain wall at the interface. (b) Interface mode dispersion $\hbar\omega$ as a function of in-plane momenta (k_x, k_z) . (c) Energy difference between the lowest bulk mode and the next lowest mode $\hbar\Delta\omega = \hbar(\omega_2 - \omega_1)$. The thick white dashed lines separate Region I where the interface mode merges with the bulk modes, and Region II where the interfacial mode is below the bulk modes in energy. The thin dashed orange lines show cuts in the $k_x k_z$ plane for which we have plotted the energy dispersion in (d), (e), and (f). (d) Band dispersion at $k_x = 0$ where two interface modes (marked in red and green lines) exist. The bulk modes are highlighted in blue and shaded with a cyan region. Inset: the band crossing between the two interface modes. (e) Band dispersion at $k_x = 2.5 \text{ nm}^{-1}$ where one interface mode (red line) merges into the bulk modes for $k_z \sim [-1, 1] \text{ nm}^{-1}$ (Inset), consistent with Region I of (c). (f) Band dispersion at $k_x = k_z$ where one interface mode (red) exists. Inset: the interface mode's velocity is than that of the the bulk modes. The lowest bulk mode is shown with the dotted blue line in (d)-(f). We use $r = .8$; $s = .713$; $t = .9$ in units of $10^{-12} \text{ m}^4/\text{s}^2$ and $a = 6.75, b = 3.17, c = 1.01, d = 1.93, f = 11.02$ in units of $10^6 \text{ m}^2/\text{s}^2$.

$\Phi_a = a\theta$, $\cot\theta = \frac{u_{xx} - u_{yy}}{2u_{xy}}$, with $C_{3,4}, M_{3,4}, A_{0,4}, D$ as material parameters [40]. $|m|(\cos\Phi_a\Gamma_1 - \sin\Phi_a\Gamma_2)$ is a complex valley dependent mass term due to strain that can gap out the Dirac points, as depicted in Fig. 1(a) (ii). We consider a static strain $u_{ij}^{(0)}$ and a dynamical strain field δu_{ij} , $u_{ij} = u_{ij}^{(0)} + \delta u_{ij}$, in which the static strain is chosen only to possess non-zero $u_{xx}^{(0)} - u_{yy}^{(0)}$ and $u_{xy}^{(0)}$ while all other components are zero. Consequently, $u_{ij}^{(0)}$ can produce the Φ_a field but not the pseudo-gauge field $\mathcal{A}^{pse} = (A_0^{pse}, \mathbf{A}_a^{pse})$. We consider acoustic phonons that create a dynamical strain field δu_{ij} , leading to the pseudo-gauge field \mathcal{A}^{pse} . We notice that A_0^{pse} has the same sign for both valleys, while \mathbf{A}_a^{pse} flips its sign between two valleys, as required by time reversal \hat{T} .

Next we assume the Fermi energy is within the energy gap of the effective Hamiltonian Eq.1, so that we can integrate out the Dirac fermions and the resulting effective

action of the pseudo-gauge field \mathcal{A}^{pse} reads [46]

$$S_{ax} = \sum_{a=\pm} S_{eff,a},$$

$$S_{eff,a} = \frac{1}{32\pi^2} \int dt d^3r \Phi_a \epsilon^{\mu\nu\rho\delta} F_{\mu\nu,a} F_{\rho\delta,a}, \quad (2)$$

where $F_{\mu\nu,a} = \partial_\mu \mathcal{A}_{\nu,a}^{pse} - \partial_\nu \mathcal{A}_{\mu,a}^{pse}$. $S_{eff,a}$, $\mu, \nu = 0, 1, 2, 3$, has a similar form as the axion electrodynamics [47–49], but it is for pseudo-gauge field \mathcal{A}^{pse} connected to the strain field. Thus, $S_{eff,a}$ is expected to influence phonon dynamics. Due to time reversal \hat{T} , the axion field Φ_a has opposite signs for two valleys, and thus we dub Φ_a as the "valley axion field". The derivation for the explicit form of the total effective action S_{ax} can be found in Sec.S1 C of SM [40]. The effective action is invariant under $\hat{C}_{6z}, \hat{C}_{2x}, \hat{T}$ and \hat{I} . We can re-write the effective action in a compact form

$$S_{ax} = - \int dt d^3r (\nabla\theta \cdot \mathbf{h}), \quad (3)$$

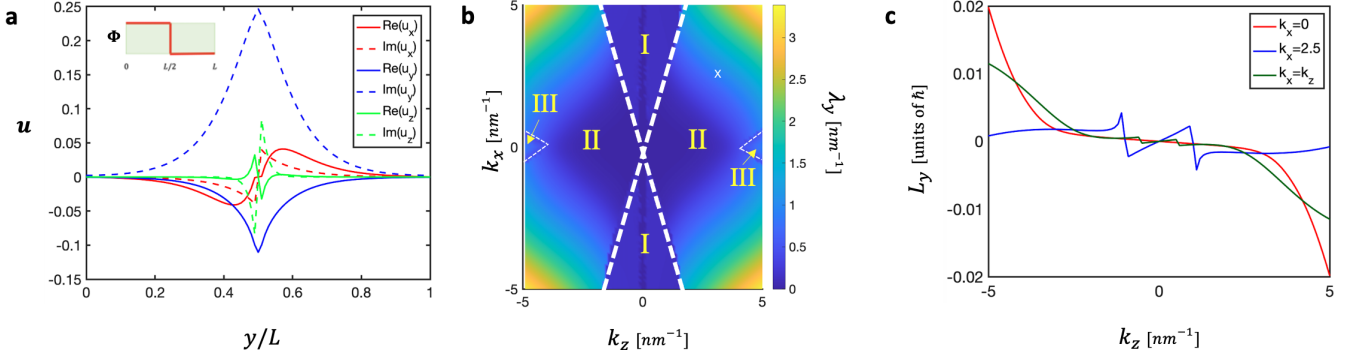


FIG. 2. (a) The spatial distribution of the real and imaginary parts of the displacement field of the interface phonon mode at point X where $(k_x, k_z) = (2.5, 3)nm^{-1}$. The u_y component (both real and imaginary) is even across the axion domain wall whereas the x and z components are odd. (b) The inverse decay length (Λ) of the dominant u_y component of the displacement as a function of (k_x, k_z) (c) The out of plane (y direction) phonon angular momentum of the interface mode at $k_x = 0$ (red) , $k_x = 2.5nm^{-1}$ (blue) and $k_x = k_z$ (dark green). We use $r = .8$; $s = .713$; $t = .9$ in units of $10^{-12}m^4/s^2$ and $a = 6.75, b = 3.17, c = 1.01, d = 1.93, f = 11.02$ in units of $10^6 m^2/s^2$.

where $h_x = -\tilde{C} (aA_0A_4M_0\partial_z u_{yz} + A_0^2\partial_y \tilde{M})$, $h_y = \tilde{C} (A_0A_4M_0\partial_z u_{xz} + A_0^2\partial_x \tilde{M})$ and $h_z = A_0A_4M_0\tilde{C} (\partial_x u_{yz} - \partial_y u_{xz})$. S_{ax} vanishes when θ is a constant and is non-zero at the θ domain wall.

Interfacial Phonon Modes at Axion Domain Wall-From the functional derivative $\delta(S_0 + S_{ax})/\delta \mathbf{u} = 0$, where S_0 is the bulk elastic action for the D_{6h} group with 5 independent elastic moduli a, b, c, d, f [50, 51] and S_{ax} is the axion term in Eq. (2), one can derive the equation of motion for the phonon displacement field \mathbf{u} as

$$H_{ph}\mathbf{u} = \rho\omega^2\mathbf{u} \quad (4)$$

, where H_{ph} is the effective phonon Hamiltonian given

$$H_{ax} = \begin{pmatrix} 0 & \frac{s}{2}k_z^2\{\partial_y, \frac{\partial\theta}{\partial y}\} & i\frac{\partial\theta}{\partial y}\alpha(k_x, k_z) \\ -\frac{s}{2}k_z^2\{\partial_y, \frac{\partial\theta}{\partial y}\} & 0 & -\frac{1}{2}(s+t)k_xk_z\{\partial_y, \frac{\partial\theta}{\partial y}\} \\ -i\frac{\partial\theta}{\partial y}\alpha(k_x, k_z) & +\frac{1}{2}(s+t)k_xk_z\{\partial_y, \frac{\partial\theta}{\partial y}\} & 0 \end{pmatrix}. \quad (5)$$

where $\alpha(k_x, k_z) = rk_z^3 - (s+t)k_x^2k_z$, $\frac{\theta_0}{2\pi^2Z}\frac{J}{2}C_3 \equiv r$, $\frac{\theta_0}{2\pi^2Z}\frac{J}{2}C_4 \equiv s$ and $\frac{\theta_0}{2\pi^2Z}A_0^2(C_3M_4 - C_4M_3) \equiv t$ with $J = -2A_0A_4M_0$ and $Z = 2A_0^2M_1k_c$. H_{ax} contains $\frac{\partial\theta}{\partial y}$, which is only non-zero at the axion domain wall.

We numerically solve the full Hamiltonian H_{ph} (Sec. S3 in SM [40]). Fig. 1(b) illustrates the anisotropic dispersion of the lowest frequency phonon mode in the \mathbf{k}_{\parallel} plane. Fig. 1(d) and (e) show the phonon dispersion along the k_z direction for $k_x = 0$ and $k_x = 2.5nm^{-1}$, respectively, while Fig. 1(f) is for phonon dispersion along the $k_x = k_z$ direction. The cyan shaded areas in Fig. 1(d)-(f) represent the dispersion of bulk phonons that

by $H_{ph} = H_{bulk} + H_{ax}$ (See Sec. S1 F and Sec. S2 A of SM [40] for the explicit form of H_{ph}). Here we assume the translation symmetry along the x and z directions, so that the in-plane momentum $\mathbf{k}_{\parallel} = (k_x, k_z)$ a good quantum number. Along the y direction, we consider a domain wall configuration for the axion field, $\Phi_a = a\theta(y) = a\pi\Theta(L/2 - y)$, where $\Theta(y)$ is the step function, $a = \pm$ and L is the system size as depicted in In Fig. 1(a) (iii). This Φ configuration can be achieved by applying a static strain $u_{xx}^{(0)} - u_{yy}^{(0)} > 0$ for $y < L/2$ and $u_{xx}^{(0)} - u_{yy}^{(0)} < 0$ for $y > L/2$ in the limit $u_{xy}^{(0)} \rightarrow 0$. Since $\Delta\Phi = \pi$, the interface is an electronic axion domain wall. By choosing the wave-function ansatz $\mathbf{u}(\mathbf{r}, t) = \mathbf{f}(y)e^{i\mathbf{k}_{\parallel}\cdot\mathbf{r}_{\parallel}}$ with $\mathbf{r}_{\parallel} = (x, z)$ and $\mathbf{k}_{\parallel} = (k_x, k_z)$, the form of the Hamiltonian H_{ax} is given by (See Sec. S2 A of SM [40])

can be obtained from the eigen-frequency of H_{bulk} . In the insets of Fig. 1(d)-(f), additional phonon modes emerge with their frequency below the bulk phonon frequency. We find one mode (red) in Fig. 1(e) and (f), and two modes (red and green) in Fig. 1(d). Fig. 1(c) depicts the frequency difference between the lowest bulk phonon frequency and the lowest phonon modes in the domain wall configuration in the \mathbf{k}_{\parallel} space, which can be divided into two regions. This frequency difference is zero in Region I, while it becomes positive in Region II, implying the existence of the modes with their frequencies below bulk phonon frequency. To further demonstrate their origin from the axion domain wall, the wave function

$\mathbf{f}(y)$ for the y -directional distribution of the displacement field at $X = (k_x, k_z) = (2.5, 3)nm^{-1}$ is depicted in Fig. 2(a). All components of displacement field \mathbf{u} decay exponentially away from the axion domain wall located at $y = L/2$, thus unambiguously demonstrating the interfacial nature of these phonon modes. The interfacial phonon wave functions $\mathbf{f}(y)$ for different momenta are further discussed in Fig. S2 of SM [40]. We can use the exponential function $\sim e^{-\lambda_y|y-L/2|}$ to fit to the solution $f_y(y)$ that exhibits the largest amplitude for different \mathbf{k}_{\parallel} , and the λ_y parameter that represents the inverse of localization length is shown as a function of \mathbf{k}_{\parallel} in Fig. 2(b). $\lambda_y = 0$ in Region I and nonzero λ_y appears in Region II and III, which means the interfacial modes only exist in Regions II and III, consistent with Fig. 1(c). Region II has one interfacial mode while Region III contains two interfacial modes. More information of these two interfacial modes can be found in Fig. S5 of SM [40]. We also find with increasing $|\mathbf{k}_{\parallel}|$, λ_y increases, so that the localization length decreases. Thus, the interfacial phonon modes become more localized for a large momentum. The existence of the interfacial phonon modes can be understood by analytically solving the eigen-equation (4) with the domain wall configuration under certain approximations. Two analytically solvable cases are considered in Sec. S2 B,C [40], and *Case I* shows the presence of interfacial modes with non-zero angular momentum, whereas *Case II* shows the presence of two interface modes, similar to the case in Fig. 1(d). Below we will only focus on *Case I* while *Case II* is discussed in Sec.S2.C of SM [40].

For *Case I*, we choose $r \neq 0$ and $s = t = 0$, such that only $\alpha = rk_z^3 \neq 0$ and take the isotropic approximation for H_{bulk} with $a = c_l^2 - c_t^2, b = d = c_t^2, c = c_l^2 - 2c_t^2, f = c_l^2$. We further assume $c_t = c_l = c_0$ such that

$$H_{ph} = \begin{pmatrix} c_0^2 k^2 - c_0^2 \partial_y^2 & 0 & -i\alpha(k_x, k_z)\delta(y) \\ 0 & c_0^2 k^2 - c_0^2 \partial_y^2 & 0 \\ i\alpha(k_x, k_z)\delta(y) & 0 & c_0^2 k^2 - c_0^2 \partial_y^2 \end{pmatrix}. \quad (6)$$

Due to the $\delta(y)$ -function, we look for exponentially localized phonon modes around $y = 0$ with the ansatz $\mathbf{u} = \sum_{\tau=1}^3 A_{\tau} e^{-\lambda_{\tau} y} \mathbf{u}_0^{\tau}(y, \lambda_{\tau})$ for $y > 0$ and $\mathbf{u} = \sum_{\tau=1}^3 B_{\tau} e^{\xi_{\tau} y} \mathbf{v}_0^{\tau}(y, \lambda_{\tau})$ for $y < 0$, where λ_{τ} and ξ_{τ} are the inverse localization lengths of mode τ for $y > 0$ and $y < 0$ respectively. \mathbf{u}_0 and \mathbf{v}_0 are the eigenmodes for $y > 0$ and $y < 0$ respectively. By matching the wave functions at the boundary at $y = 0$, we obtain 6 linear equations for the variables $A_{1,2,3}$ and $B_{1,2,3}$. By solving for the characteristic equation, we find bulk modes with $\omega = c_0 k$ ($k = \sqrt{k_x^2 + k_z^2}$) and an interfacial mode with $\omega = [(c_0 k)^2 - (\alpha(k_x, k_z)/c_0)^2]^{1/2}$. The eigen-vector of the interfacial phonon mode is $\mathbf{u} = N e^{-\lambda|y|} (\text{sgn}(\alpha), 0, -i)^T$ with the normalization factor N and the inverse localization length $\lambda = |\alpha(k_x, k_z)|/c_0^2$. This interfacial phonon mode is circularly polarized and the corresponding phonon angular momentum, defined by $l_i = \hbar \mathbf{u}_0^{\dagger} M_i \mathbf{u}_0$ where $i = x, y, z$ and $(M_i)_{jk} = (-i)\epsilon_{ijk}$ [52, 53], has

non-zero y -component, $l_y = \text{sgn}(\alpha)\hbar = \text{sgn}k_z\hbar$. The quantized angular momentum l_y is a consequence of the isotropic approximation. For a more realistic situation, we numerically evaluate the angular momentum of the interfacial phonon modes, as depicted in Fig. 2(c), in which l_y strongly depends on k_z and increases rapidly for a large k_z . l_y changes its sign for opposite momentum k_z and thus reveals a helical nature due to time reversal \hat{T} [54, 55]. More information of phonon angular momentum is provided in Fig. S3 and S4, and discussed in Sec. S5 of SM [40]. This phonon helicity can be probed via temperature gradient induced phonon angular momentum [53–55], and our numerical and symmetry analysis suggested the z -directional temperature gradient can induce the y -directional angular momentum l_y via the axion term, and this response is absent if there is no axion term, as discussed in Sec.S5.B and C of SM (Fig. S9b) [40]. With increasing $|\mathbf{k}_{\parallel}|$, the dispersion of the interfacial phonon mode generally exhibits a maximum at a certain momentum and then its frequency drops down. With further increasing \mathbf{k}_{\parallel} , the phonon frequency can drop to zero and then become imaginary, implying a lattice instability. Nevertheless, our effective action of acoustic phonon dynamics is only valid for the momentum within the first Brillouin zone and breaks down closer to the Brillouin zone boundary (roughly at $\sim 10nm^{-1}$), so we restrict our in-plane momenta to be $5nm^{-1}$. Within this range of momenta and based on the current material parameters, the axion term H_{ax} is not strong enough for a lattice instability. It is well-known that a surface acoustic wave can exist at the surface of an elastic material (described by the phonon Hamiltonian H_{bulk} with a stress-free boundary condition), even in the absence of the valley axion term [41]. The presence of axion term will also strongly affect the surface acoustic wave (See Sec. S4 of SM [40]).

Conclusion - In this work, we demonstrate the existence of the interfacial phonon modes localized at the domain wall between two regions with different valley axion parameters, which originates from the electron-phonon interaction in the gapped Dirac semimetal model. Although our model is derived for Na_3Bi , this mechanism can be generalized to other Dirac materials. The key requirement is that the low-energy Dirac Hamiltonian should be located at generic momenta that are not time-reversal-invariant, as the complex mass and the pseudo-gauge field terms in Eq. (1) generally break \hat{T} . Given this requirement, the existing Dirac materials, Na_3Bi and Cd_3As_2 [38, 39] may host interfacial phonon modes from our mechanism. We notice that the interfacial phonon modes have been previously observed in epitaxial Si-Ge interface via a combination of Raman spectroscopy and high-energy-resolution electron energy-loss spectroscopy (EELS) in a scanning transmission electron microscope[56], and in epitaxial cubic boron nitride/diamond heterointerface using 4D EELS [57], and similar experimental probes may be implemented to detect the interfacial phonon modes. The unique phonon angular momentum distribution in the momen-

tum space[53–55] may help to distinguish this mechanism of interfacial phonon modes from other origins [56, 57]. Our mechanism can also be applied to magnetic topological materials, e.g. MnBi_2Te_4 , even though the Dirac Hamiltonian is located at a high-symmetry momenta [58–60] but \hat{T} is already broken by its intrinsic magnetism.

One may also expect interfacial magnon mode in these magnetic topological materials due to electron-magnon interaction.

Acknowledgement - We acknowledge helpful discussions with Z. Bi and N. Kalyanapuram. A.C. and C.-X.L. acknowledge support from NSF grant via the grant number DMR-2241327.

-
- [1] X.-L. Qi and S.-C. Zhang, *Reviews of Modern Physics* **83**, 1057 (2011).
- [2] M. Z. Hasan and C. L. Kane, *Reviews of modern physics* **82**, 3045 (2010).
- [3] B. Yan and S.-C. Zhang, *Reports on Progress in Physics* **75**, 096501 (2012).
- [4] B. J. Wieder, B. Bradlyn, J. Cano, Z. Wang, M. G. Vergniory, L. Elcoro, A. A. Soluyanov, C. Felser, T. Neupert, N. Regnault, *et al.*, *Nature Reviews Materials* **7**, 196 (2022).
- [5] S. Ryu and Y. Hatsugai, *Physical review letters* **89**, 077002 (2002).
- [6] A. P. Schnyder, S. Ryu, A. Furusaki, and A. W. Ludwig, *Physical Review B* **78**, 195125 (2008).
- [7] R. S. Mong and V. Shivamoggi, *Physical Review B* **83**, 125109 (2011).
- [8] S. Ryu, A. P. Schnyder, A. Furusaki, and A. W. Ludwig, *New Journal of Physics* **12**, 065010 (2010).
- [9] Y. Tanaka, M. Sato, and N. Nagaosa, *Journal of the Physical Society of Japan* **81**, 011013 (2011).
- [10] A. Kitaev, in *AIP conference proceedings*, Vol. 1134 (American Institute of Physics, 2009) pp. 22–30.
- [11] Y. Hatsugai, *Solid state communications* **149**, 1061 (2009).
- [12] L. Lu, J. D. Joannopoulos, and M. Soljačić, *Nature photonics* **8**, 821 (2014).
- [13] T. Ozawa, H. M. Price, A. Amo, N. Goldman, M. Hafezi, L. Lu, M. C. Rechtsman, D. Schuster, J. Simon, O. Zilberberg, *et al.*, *Reviews of Modern Physics* **91**, 015006 (2019).
- [14] Y. Liu, X. Chen, and Y. Xu, *Advanced Functional Materials* **30**, 1904784 (2020).
- [15] H. Chen, W. Zhang, Q. Niu, and L. Zhang, *2D Materials* **6**, 012002 (2018).
- [16] X.-Q. Chen, J. Liu, and J. Li, *The Innovation* **2** (2021).
- [17] F. Zhuo, J. Kang, A. Manchon, and Z. Cheng, *Advanced Physics Research*, 2300054 (2023).
- [18] P. A. McClarty, *Annual Review of Condensed Matter Physics* **13**, 171 (2022).
- [19] E. J. Bergholtz, J. C. Budich, and F. K. Kunst, *Reviews of Modern Physics* **93**, 015005 (2021).
- [20] M. J. Gilbert, *Communications Physics* **4**, 70 (2021).
- [21] S. Zheng, G. Duan, and B. Xia, *Applied Sciences* **12**, 1987 (2022).
- [22] G. Ma, M. Xiao, and C. T. Chan, *Nature Reviews Physics* **1**, 281 (2019).
- [23] X. Mao and T. C. Lubensky, *Annual Review of Condensed Matter Physics* **9**, 413 (2018).
- [24] P. Thalmeier, *Physical Review B* **83**, 125314 (2011).
- [25] S. Giraud and R. Egger, *Physical Review B* **83**, 245322 (2011).
- [26] S. Giraud, A. Kundu, and R. Egger, *Physical Review B* **85**, 035441 (2012).
- [27] G. Huang, *Europhysics Letters* **100**, 17001 (2012).
- [28] V. Parente, A. Tagliacozzo, F. Von Oppen, and F. Guinea, *Physical Review B* **88**, 075432 (2013).
- [29] I. Garate, *Physical Review Letters* **110**, 046402 (2013).
- [30] T. Karzig, C.-E. Bardyn, N. H. Lindner, and G. Refael, *Physical Review X* **5**, 031001 (2015).
- [31] W. Liu, Z. Ji, Y. Wang, G. Modi, M. Hwang, B. Zheng, V. J. Sorger, A. Pan, and R. Agarwal, *Science* **370**, 600 (2020).
- [32] S. Klembt, T. Harder, O. Egorov, K. Winkler, R. Ge, M. Bandres, M. Emmerling, L. Worschech, T. Liew, M. Segev, *et al.*, *Nature* **562**, 552 (2018).
- [33] G. Hu, Q. Ou, G. Si, Y. Wu, J. Wu, Z. Dai, A. Krasnok, Y. Mazor, Q. Zhang, Q. Bao, *et al.*, *Nature* **582**, 209 (2020).
- [34] M. Li, I. Sinev, F. Benimetskiy, T. Ivanova, E. Khestanova, S. Kiriushchikina, A. Vakulenko, S. Guddala, M. Skolnick, V. M. Menon, *et al.*, *Nature communications* **12**, 4425 (2021).
- [35] Y. V. Kartashov and D. V. Skryabin, *Physical review letters* **122**, 083902 (2019).
- [36] Z. Liu, B. Zhou, Y. Zhang, Z. Wang, H. Weng, D. Prabhakaran, S.-K. Mo, Z. Shen, Z. Fang, X. Dai, *et al.*, *Science* **343**, 864 (2014).
- [37] J. Xiong, S. K. Kushwaha, T. Liang, J. W. Krizan, M. Hirschberger, W. Wang, R. J. Cava, and N. P. Ong, *Science* **350**, 413 (2015).
- [38] Z. Wang, Y. Sun, X.-Q. Chen, C. Franchini, G. Xu, H. Weng, X. Dai, and Z. Fang, *Physical Review B* **85**, 195320 (2012).
- [39] Z. Wang, H. Weng, Q. Wu, X. Dai, and Z. Fang, *Physical Review B* **88**, 125427 (2013).
- [40] See Supplementary Material at [URL]. In Sec. S1, we present the effective theory of Na_3Bi based on the symmetry properties of D_{6h} symmetry group with relevant material parameters. We derive the effective action S_{eff} and discuss the symmetry properties of S_{eff} . We close Sec. S1 with the bulk action and deriving the equation of motion in the presence of the axion term. In Sec. S2, we provide details of the analytical solutions for *Case I* and *Case II*. In Sec. S3, we provide the framework for our numerical calculations and elaborate on some of the numerical features presented in the main text. In Sec. S4, we perform detailed calculations to show the influence of the axion term on the already present surface modes of an elastic material with an open boundary. Lastly, in Sec. S5, we present the formalism for the phonon angular momentum and describe probing the helical nature of the interface phonon modes using a temperature gradient.
- [41] L. D. Landau, E. M. Lifshitz, A. M. Kosevich, and L. P. Pitaevskii, *Theory of elasticity: volume 7*, Vol. 7 (Else-

- vier, 1986).
- [42] F. de Juan, J. L. Manes, and M. A. Vozmediano, *Physical Review B* **87**, 165131 (2013).
- [43] D. Pikulin, A. Chen, and M. Franz, *Physical Review X* **6**, 041021 (2016).
- [44] R. Ilan, A. G. Grushin, and D. I. Pikulin, *Nature Reviews Physics* **2**, 29 (2020).
- [45] J. Yu and C.-X. Liu, in *Semiconductors and Semimetals*, Vol. 108 (Elsevier, 2021) pp. 195–224.
- [46] J. Yu, B. J. Wieder, and C.-X. Liu, *Physical Review B* **104**, 174406 (2021).
- [47] F. Wilczek, *Physical review letters* **58**, 1799 (1987).
- [48] A. Sekine and K. Nomura, *Journal of Applied Physics* **129** (2021).
- [49] D. M. Nenko, C. A. Garcia, J. Gooth, C. Felser, and P. Narang, *Nature Reviews Physics* **2**, 682 (2020).
- [50] M. De Jong, W. Chen, T. Angsten, A. Jain, R. Notestine, A. Gamst, M. Sluiter, C. Krishna Ande, S. Van Der Zwaag, J. J. Plata, *et al.*, *Scientific data* **2**, 1 (2015).
- [51] X.-X. Dong, J.-X. Chen, Y. Wang, Z.-L. Lv, and H.-Y. Wang, *Materials Research Express* **6**, 076308 (2019).
- [52] L. Zhang and Q. Niu, *Physical Review Letters* **112**, 085503 (2014).
- [53] M. Hamada, E. Minamitani, M. Hirayama, and S. Murakami, *Physical review letters* **121**, 175301 (2018).
- [54] L.-H. Hu, J. Yu, I. Garate, and C.-X. Liu, *Physical review letters* **127**, 125901 (2021).
- [55] C.-X. Liu, *Physical Review B* **106**, 115102 (2022).
- [56] Z. Cheng, R. Li, X. Yan, G. Jernigan, J. Shi, M. E. Liao, N. J. Hines, C. A. Gadre, J. C. Idrobo, E. Lee, *et al.*, *Nature communications* **12**, 6901 (2021).
- [57] R. Qi, R. Shi, Y. Li, Y. Sun, M. Wu, N. Li, J. Du, K. Liu, C. Chen, J. Chen, *et al.*, *Nature* **599**, 399 (2021).
- [58] M. M. Otrokov, I. I. Klimovskikh, H. Bentmann, D. Estyunin, A. Zeugner, Z. S. Aliev, S. Gaß, A. Wolter, A. Koroleva, A. M. Shikin, *et al.*, *Nature* **576**, 416 (2019).
- [59] D. Zhang, M. Shi, T. Zhu, D. Xing, H. Zhang, and J. Wang, *Physical review letters* **122**, 206401 (2019).
- [60] J. Li, Y. Li, S. Du, Z. Wang, B.-L. Gu, S.-C. Zhang, K. He, W. Duan, and Y. Xu, *Science Advances* **5**, eaaw5685 (2019).
- [61] R. Winkler, S. Papadakis, E. De Poortere, and M. Shayegan, *Spin-orbit coupling in two-dimensional electron and hole systems*, Vol. 41 (Springer, 2003).
- [62] W. Kress and F. W. de Wette, *Surface phonons* (Springer, 1991).
- [63] S. M. Girvin and K. Yang, *Modern condensed matter physics* (Cambridge University Press, 2019).

CONTENTS

References	5
S1. Effective theory of Na_3Bi	2
A. Symmetry properties of D_{6h}	2
B. Effective Hamiltonian	2
C. Effective action S_{ax}	4
D. Symmetries of S_{ax}	6
1. Six-fold rotation: \hat{C}_{6z}	6
2. Two-fold rotation \hat{C}_{2x}	7
3. Reflection m_x	7
E. Bulk action	8
F. Equation of motion with the Axion term	9
S2. Analytic solution of Axion domain wall modes	11
A. Bulk axion domain wall	11
B. Case I: α term	11
C. Case II: only $s \neq 0$	12
S3. Numerical method	15
A. H_0 term	15
B. H_1 term	15
C. Numerical Results	16
S4. Surface phonon modes	17
A. xz plane configuration	18
B. Isotropic approximation for the bulk action without the Axion term	18
C. Numerical method	20
D. Numerical Results	21
E. Hermiticity of the Hamiltonian	22
1. Hermiticity of Eq(57)	22
2. Hermiticity of Eq(94)	23
S5. Angular momentum of phonon modes	23
A. Derivation of total angular momentum for a lattice configuration	23
B. Effect of thermal gradient	24
C. Symmetry properties of the response tensor α_{ij}	26
References	26

Supplementary Materials for "Localized interfacial phonon modes at the Electronic Axion Domain Wall"

S1. EFFECTIVE THEORY OF Na_3Bi

A. Symmetry properties of D_{6h}

The crystal point group for Na_3Bi is D_{6h} , generated by 6-fold rotation about the z-axis \hat{C}_{6z} , 2-fold rotation about the x-axis, \hat{C}_{2x} and inversion \hat{I} . Γ are the irreducible representations of the group. The \pm in Γ^\pm denotes even (+) or odd (-) under inversion. The character table of D_{6h} is given in Table S1 :

D_{6h}	E	$2C_{6z}$	$2C_{3z}$	C_{2z}	$2C_{2x}$	$2C_{2y}$	I	$2IC_{6z}$	$2IC_{3z}$	IC_{2z}	$3IC_{2x}$	$3IC_{2y}$
$\tilde{\Gamma}_1^\pm$	1	1	1	1	1	1	± 1	± 1	± 1	± 1	± 1	± 1
$\tilde{\Gamma}_2^\pm$	1	1	1	1	-1	-1	± 1	± 1	± 1	± 1	∓ 1	∓ 1
$\tilde{\Gamma}_3^\pm$	1	-1	1	-1	1	-1	± 1	∓ 1	± 1	∓ 1	± 1	∓ 1
$\tilde{\Gamma}_4^\pm$	1	-1	1	-1	-1	1	± 1	∓ 1	± 1	∓ 1	∓ 1	± 1
$\tilde{\Gamma}_5^\pm$	2	1	-1	-2	0	0	± 2	± 1	∓ 1	∓ 2	0	0
$\tilde{\Gamma}_6^\pm$	2	-1	-1	2	0	0	± 2	∓ 1	∓ 1	± 2	0	0

TABLE S1. Character Table of D_{6h} group

The four-by-four Dirac matrices are defined as

$$\begin{aligned}
 \Gamma_i &= \sigma_i \otimes \tau_1, \Gamma_4 = I \otimes \tau_2, \Gamma_5 = I \otimes \tau_3 \\
 \Gamma_{ij} &= \epsilon_{ijk} \sigma_k \otimes I, \Gamma_{i4} = \sigma_i \otimes \tau_3, \Gamma_{i5} = -\sigma_i \otimes \tau_2 \\
 \Gamma_{45} &= I \otimes \tau_1; i, j = 1, 2, 3
 \end{aligned} \tag{7}$$

where I labels the identity matrix and σ, τ are two sets of Pauli matrices representing spin and orbital degrees of freedoms, respectively. On the basis wavefunction $|s \uparrow\rangle, |p_+ \uparrow\rangle, |s \downarrow\rangle, |p_- \downarrow\rangle$, the symmetry operators are given by

$$\hat{C}_{6z} = e^{i\frac{\pi}{6}(\sigma_3 \otimes (2I - \tau_3))}, \hat{C}_{2x} = i\sigma_1 \otimes \tau_3, \hat{I} = I \otimes \tau_3, \hat{T} = (i\sigma_2 \otimes I) K. \tag{8}$$

The representations of the Dirac Γ -matrices, the momenta \mathbf{k} and the strain tensors, as well as their behavior under time reversal T are given in Table S2. The direct products of irreps can be found in Table S3. The above irreps can be even or odd ($\tilde{\Gamma}^\pm$) under inversion and be $T = \pm$ under time reversal. The direct product of such irreps follow simple multiplication e.g. $\tilde{\Gamma}_5^+(T = +) \times \tilde{\Gamma}_6^-(T = -) = \tilde{\Gamma}_3^-(T = -) + \tilde{\Gamma}_4^-(T = -) + \tilde{\Gamma}_5^-(T = -)$.

B. Effective Hamiltonian

The low energy effective Hamiltonian of Na_3Bi reads [38]

$$H_{Na_3Bi} = C_0 + C_1 k_z^2 + C_2 k_{||}^2 + (M_0 + M_1 k_z^2 + M_2 k_{||}^2) \Gamma_5 + A_0 (k_x \Gamma_3 - k_y \Gamma_4), \tag{9}$$

in the basis $|s \uparrow\rangle, |p_+ \uparrow\rangle, |s \downarrow\rangle, |p_- \downarrow\rangle$, with basis of the form $|\alpha, \sigma\rangle, \alpha = s, p_\pm$ represents the orbital degree of freedom and $\sigma = \uparrow, \downarrow$ is the spin degree of freedom. $C_{0,1,2}, M_{0,1,2}, A_0$ are material dependent materials [38, 50, 51] given in Table S4

We next introduce the Hamiltonian to describe the electron-strain coupling via symmetry construction. We define the strain tensor as $u_{ij} = \frac{1}{2}(\partial_i u_j + \partial_j u_i)$. Using the tables in Section S1 A, we construct the minimal Hamiltonian in the presence of a strain perturbation as [61]

$$\begin{aligned}
 H_{str} &= [C_3 u_{zz} + C_4 (u_{xx} + u_{yy})] \mathbb{I} + [M_3 u_{zz} + M_4 (u_{xx} + u_{yy})] \Gamma_5 + [A_1 u_{zz} + A_2 (u_{xx} + u_{yy})] (k_x \Gamma_3 - k_y \Gamma_4) \\
 &+ A_3 (k_x (u_{xx} - u_{yy}) + 2k_y u_{xy}) \Gamma_3 - A_3 (2k_x u_{xy} - k_y (u_{xx} - u_{yy})) \Gamma_4 + A_4 k_z (u_{xz} \Gamma_3 - u_{yz} \Gamma_4) \\
 &+ A_5 (k_x u_{yz} + k_y u_{xz}) \Gamma_2 + A_5 (k_x u_{xz} - k_y u_{yz}) \Gamma_1 + D k_z (2u_{xy} \Gamma_2 + (u_{xx} - u_{yy}) \Gamma_1)
 \end{aligned} \tag{10}$$

Representation T		
$\{\Gamma_1, \Gamma_2\}$	$\tilde{\Gamma}_6^-$	—
$\{\Gamma_3, \Gamma_4\}$	$\tilde{\Gamma}_5^-$	—
$\Gamma_5, \mathbb{I} \otimes \mathbb{I}$	$\tilde{\Gamma}_1^+$	+
$\{\Gamma_{12}\}, \{\Gamma_{34}\}$	$\tilde{\Gamma}_2^+$	—
$\{\Gamma_{35}, \Gamma_{45}\}$	$\tilde{\Gamma}_5^-$	+
$\{\Gamma_{15}, \Gamma_{25}\}$	$\tilde{\Gamma}_6^-$	+
$\{\Gamma_{23} + \Gamma_{14}, \Gamma_{31} + \Gamma_{24}\}$	$\tilde{\Gamma}_5^+$	—
$\{\Gamma_{23} - \Gamma_{14}, \Gamma_{31} - \Gamma_{24}\}$	$\tilde{\Gamma}_5^+$	—
$\{k_x, k_y\}$	$\tilde{\Gamma}_5^-$	—
$\{k_z\}, \{k_z^3\}$	$\tilde{\Gamma}_2^-$	—
$\{1\}, \{k_x^2\}, \{k_z^2\}$	$\tilde{\Gamma}_1^+$	+
$\{k_x^2 - k_y^2, 2k_x k_y\}$	$\tilde{\Gamma}_6^+$	+
$\{k_x k_x^2, k_y k_y^2\}$	$\tilde{\Gamma}_5^-$	—
$\{u_{xz}, u_{yz}\}$	$\tilde{\Gamma}_5^+$	+
$\{u_{zz}\}, \{u_{xx} + u_{yy}\}$	$\tilde{\Gamma}_1^+$	+
$\{u_{xy}, u_{xx} - u_{yy}\}$	$\tilde{\Gamma}_6^+$	+

TABLE S2. Representations of Γ , \mathbf{k} and u_{ij}

$\tilde{\Gamma}_1$	$\tilde{\Gamma}_2$	$\tilde{\Gamma}_3$	$\tilde{\Gamma}_4$	$\tilde{\Gamma}_5$	$\tilde{\Gamma}_6$	
$\tilde{\Gamma}_1$	$\tilde{\Gamma}_1$	$\tilde{\Gamma}_2$	$\tilde{\Gamma}_3$	$\tilde{\Gamma}_4$	$\tilde{\Gamma}_5$	$\tilde{\Gamma}_6$
$\tilde{\Gamma}_2$	$\tilde{\Gamma}_2$	$\tilde{\Gamma}_1$	$\tilde{\Gamma}_4$	$\tilde{\Gamma}_3$	$\tilde{\Gamma}_5$	$\tilde{\Gamma}_6$
$\tilde{\Gamma}_3$	$\tilde{\Gamma}_3$	$\tilde{\Gamma}_4$	$\tilde{\Gamma}_1$	$\tilde{\Gamma}_2$	$\tilde{\Gamma}_6$	$\tilde{\Gamma}_5$
$\tilde{\Gamma}_4$	$\tilde{\Gamma}_4$	$\tilde{\Gamma}_3$	$\tilde{\Gamma}_2$	$\tilde{\Gamma}_1$	$\tilde{\Gamma}_6$	$\tilde{\Gamma}_5$
$\tilde{\Gamma}_5$	$\tilde{\Gamma}_5$	$\tilde{\Gamma}_5$	$\tilde{\Gamma}_6$	$\tilde{\Gamma}_6$	$\tilde{\Gamma}_1 + \tilde{\Gamma}_2 + \tilde{\Gamma}_6$	$\tilde{\Gamma}_3 + \tilde{\Gamma}_4 + \tilde{\Gamma}_5$
$\tilde{\Gamma}_6$	$\tilde{\Gamma}_6$	$\tilde{\Gamma}_6$	$\tilde{\Gamma}_5$	$\tilde{\Gamma}_5$	$\tilde{\Gamma}_3 + \tilde{\Gamma}_4 + \tilde{\Gamma}_5$	$\tilde{\Gamma}_1 + \tilde{\Gamma}_2 + \tilde{\Gamma}_6$

TABLE S3. Direct products of the irreducible representations of the D_{6h} group

where we have kept all the terms up to the linear order in both \mathbf{k} and \mathbf{u} , as well as the order of $k_i u_{jk}$ with $i, j, k = x, y, z$. The Dirac points of H_{Na_3Bi} are located at the momenta $(0, 0, ak_c)$, where $k_c = \sqrt{-\frac{M_0}{M_1}}$ and $a = \pm$ are dubbed two "valleys" below. We project both the Hamiltonians $H_{Na_3Bi} + H_{str}$ into the subspace formed by four eigen-states at the Dirac points of H_{Na_3Bi} at $(0, 0, ak_c)$. We keep all the terms up to the linear order in \mathbf{k} . The total effective Hamiltonian after the projection is given by $\tilde{H} = \sum_a \tilde{H}_a$. The valley dependent term is given by

$$\begin{aligned}
\tilde{H}_a = & [C_3 u_{zz} + C_4 (u_{xx} + u_{yy})] \mathbb{I} + A_0 \left[k_x + a \frac{A_4}{A_0} k_c u_{xz} \right] \Gamma_3 - A_0 \left[k_y + a \frac{A_4}{A_0} k_c u_{yz} \right] \Gamma_4 \\
& + 2a M_1 k_c \left[k_z + \frac{a}{2M_1 k_c} (M_3 u_{zz} + M_4 (u_{xx} + u_{yy})) \right] \Gamma_5 + 2a D k_c u_{xy} \Gamma_2 \\
& + D k_c a (u_{xx} - u_{yy}) \Gamma_1.
\end{aligned} \tag{11}$$

In \tilde{H}_a , the z component of Fermi velocity given by $2a M_1 k_c$ is dependent on the valley index a . In order to remove this valley dependence, we perform a unitary transformation for $H_{a=+}$ with $U = \Gamma_{15}$, but not for $H_{a=-}$, since $H_{a=-}$ and $H_{a=+}$ are independent of each other. Thus, $H_{a=-} = \tilde{H}_{a=-}$ and $H_{a=+} = U \tilde{H}_{a=+} U^{-1}$. We can rewrite the valley dependent Hamiltonian as

$$\begin{aligned}
H_a = & [C_3 u_{zz} + C_4 (u_{xx} + u_{yy})] \mathbb{I} + A_0 \left[k_x + a \frac{A_4}{A_0} k_c u_{xz} \right] \Gamma_3 - A_0 \left[k_y + a \frac{A_4}{A_0} k_c u_{yz} \right] \Gamma_4 \\
& - 2M_1 k_c \left[k_z + \frac{a}{2M_1 k_c} (M_3 u_{zz} + M_4 (u_{xx} + u_{yy})) \right] \Gamma_5 + D k_c \left[(u_{xx} - u_{yy}) \Gamma_1 - 2a u_{xy} \Gamma_2 \right]
\end{aligned} \tag{12}$$

C_0	$-0.06382eV$	C_1	$8.7536eV\hat{A}^2$	C_2	$-8.4008eV\hat{A}^2$
M_0	-0.08686 eV	M_1	$10.6424eV\hat{A}^2$	M_2	$10.3610eV\hat{A}^2$
A_0	$2.4598eV\hat{A}$	a	$6.75 \times 10^6 m^2/s^2$	b	$3.17 \times 10^6 m^2/s^2$
c	$1.01 \times 10^6 m^2/s^2$	d	$1.93 \times 10^6 m^2/s^2$	f	$11.02 \times 10^6 m^2/s^2$

TABLE S4. Materials parameters for Na_3Bi

The strain perturbation has induced a pseudo-gauge field of the form $(A_0^{pse}, \vec{A}^{pse})$ with

$$\begin{aligned} A_0^{pse} &= C_3 u_{zz} + C_4 (u_{xx} + u_{yy}) \\ \vec{A}^{pse} &= -a \left[-A_4 k_c u_{xz}, A_4 k_c u_{yz}, M_3 u_{zz} + M_4 (u_{xx} + u_{yy}) \right] \end{aligned} \quad (13)$$

C. Effective action S_{ax}

The above Dirac type of Hamiltonian may be re-written as a Lagrangian density

$$\mathcal{L} = \sum_{a=\pm} \mathcal{L}_a = \sum_{a=\pm} \bar{\psi}_a [i\rlap{\not{\partial}} - e\vec{A}_a^{pse} + |m| (\cos \Phi_a I + \sin \Phi_a \gamma^5)] \psi_a \quad (14)$$

where $\bar{\psi}_a = \psi^\dagger \gamma^0$, $\rlap{\not{\partial}}_a = \gamma^\mu \partial_{\mu,a}$, $\vec{A}_a^{pse} = \gamma^\mu A_{\mu,a}^{pse}$, $\partial_{0,a} = \partial_t$, $\partial_{1,a} = A_0 \partial_x$, $\partial_{2,a} = -A_0 \partial_y$, $\partial_{3,a} = -2M_1 k_c \partial_z$. The mass term is given by $|m| = Dk_c ((2u_{xy})^2 + (u_{xx} - u_{yy})^2)^{1/2}$. We have $\gamma^0 = \Gamma_1$, $\gamma^1 = \Gamma_1 \Gamma_3 = i\Gamma_{13}$, $\gamma^2 = \Gamma_1 \Gamma_4 = i\Gamma_{14}$, $\gamma^3 = \Gamma_1 \Gamma_5 = i\Gamma_{15}$, $\gamma^5 = i\gamma^0 \gamma^1 \gamma^2 \gamma^3 = -i\sigma_3 \otimes I$, $\Gamma_2 = -i\gamma^0 \gamma^5 = \sigma_2 \otimes \tau_1$,

$$\Phi_a = a\theta; \quad \cot \theta = \frac{u_{xx} - u_{yy}}{2u_{xy}}. \quad (15)$$

The corresponding Hamiltonian form of the above Lagrangian is

$$H = \sum_{a=1}^2 H_a = \sum_{a=1}^2 \psi_a^\dagger \left[A_0^{pse} + \gamma^0 \gamma^j (-i\partial_j + A_j^{pse}) - |m| \gamma^0 (\cos \Phi_a I + \sin \Phi_a \gamma^5) \right] \psi_a. \quad (16)$$

The above Hamiltonian can be compared with the Hamiltonian $H_a(\{u\} = 0)$ in Eq. (12) to determine the forms of γ 's in terms of Γ 's. Three linear-momentum terms can be uniquely fixed by requiring

$$\gamma^0 \gamma^1 = \Gamma_3 = \sigma_3 \otimes \tau_1 \quad (17)$$

$$\gamma^0 \gamma^2 = \Gamma_4 = I \otimes \tau_2 \quad (18)$$

$$\gamma^0 \gamma^3 = \Gamma_5 = I \otimes \tau_3. \quad (19)$$

There are still two possible choices to assign the two mass terms when comparing Eq(16) with Eq. (12). As the mirror symmetry about yz plane, m_x , is preserved for the model Hamiltonian of Na_3Bi , two mass terms in Eqs.(16) and (12) should be transformed in the same way. In the Na_3Bi basis of the Hamiltonian (12), we have $\hat{m}_x = \hat{I}C_{2x} = (I \otimes \tau_3)(i\sigma_1 \otimes \tau_3) = i\sigma_1 \otimes I$. Under \hat{m}_x , Γ_1 transforms as:

$$m_x^{-1} \Gamma_1 m_x = -i(\sigma_1 \otimes I)(\sigma_1 \otimes \tau_1)i(\sigma_1 \otimes I) = \Gamma_1 \quad (20)$$

Similarly, Γ_2 transforms as:

$$m_x^{-1} \Gamma_2 m_x = -i(\sigma_1 \otimes I)(\sigma_2 \otimes \tau_1)i(\sigma_1 \otimes I) = -\Gamma_2 \quad (21)$$

In the spinor basis of the Dirac equation, we have $\hat{I} \equiv \gamma^0$ and $\hat{C}_{2x} = e^{-i\frac{\pi}{2}\sigma_{23}} = -i\sigma_{23} \equiv S$ where $\sigma_{23} = \frac{i}{2}[\gamma^2, \gamma^3]$. We have,

$$\begin{aligned}
\hat{m}_x^{-1}\gamma^0\hat{m}_x &= \left(\hat{I}\hat{C}_{2x}\right)^{-1}\gamma^0\left(\hat{I}\hat{C}_{2x}\right) = (\gamma^0 S)^{-1}\gamma^0(\gamma^0 S) = S^{-1}\gamma^0\gamma^0\gamma^0 S = S^{-1}\gamma^0 S \\
&= \left(\cos\frac{\pi}{2} + i\sin\frac{\pi}{2}\sigma_{23}\right)\gamma^0\left(\cos\frac{\pi}{2} - i\sin\frac{\pi}{2}\sigma_{23}\right) = \sigma_{23}\gamma^0\sigma_{23} \\
&= \frac{i}{2}[\gamma^2, \gamma^3]\gamma^0\frac{i}{2}[\gamma^2, \gamma^3] = -\frac{1}{4}(\gamma^2\gamma^3 - \gamma^3\gamma^2)\gamma^0(\gamma^2\gamma^3 - \gamma^3\gamma^2) \\
&= -\frac{1}{4}\gamma^0(\gamma^2\gamma^3 - \gamma^3\gamma^2)^2 = -\frac{1}{4}\gamma^0(-4I) \\
&= \gamma^0
\end{aligned} \tag{22}$$

Since γ_0 is invariant under $\hat{I}\hat{C}_{2x}$, we must have $\gamma^0 = \Gamma_1$. Similarly, one can show $\hat{m}_x^{-1}\gamma^0\gamma^5\hat{m}_x = -\gamma^0\gamma^5$ so that $\gamma^0\gamma^5 = \Gamma_2$.

With the above Lagrangian Eq. (14), we can derive the total effective action as $S_{ax} = \sum_a S_{eff,a}$ by integrating out the Dirac fermions [46] via the path integral form

$$e^{iS_{eff,a}} = \int D\bar{\psi}_a D\psi_a \exp\left[i\int dt d^3r \mathcal{L}_a\right], \tag{23}$$

where

$$S_{eff,a} = \frac{1}{32\pi^2} \int dt d^3r \Phi_a \epsilon^{\mu\nu\rho\delta} F_{\mu\nu,a}^{pse} F_{\rho\delta,a}^{pse} \tag{24}$$

and $F_{\mu\nu,a}^{pse} = \partial_\mu A_{\nu,a}^{pse} - \partial_\nu A_{\mu,a}^{pse}$. Since we only discuss the pseudo-gauge field, we drop the upper index "pse". We define $\tilde{C} = C_3 u_{zz} + C_4(u_{xx} + u_{yy})$, $\tilde{M} = M_3 u_{zz} + M_4(u_{xx} + u_{yy})$, $\partial_1 = A_0 \partial_x$, $\partial_2 = -A_0 \partial_y$ and $\partial_3 = -2M_1 k_c \partial_z$, and find

$$\begin{aligned}
F_{01,a} &= \dot{A}_{1,a} - \partial_1 A_{0,a} = \left[a A_4 k_c \dot{u}_{xz} - A_0 \partial_x \tilde{C} \right] \\
F_{02,a} &= \dot{A}_{2,a} - \partial_2 A_{0,a} = \left[-a A_4 k_c \dot{u}_{yz} + A_0 \partial_y \tilde{C} \right] \\
F_{03,a} &= \dot{A}_{3,a} - \partial_3 A_{0,a} = \left[-a \dot{M} + 2M_1 k_c \partial_z \tilde{C} \right] \\
F_{12,a} &= \partial_1 A_{2,a} - \partial_2 A_{1,a} = -a A_0 A_4 k_c \left[\partial_x u_{yz} - \partial_y u_{xz} \right] \\
F_{23,a} &= \partial_2 A_{3,a} - \partial_3 A_{2,a} = a \left[A_0 \partial_y \tilde{M} - 2A_4 M_1 k_c^2 \partial_z u_{yz} \right] \\
F_{13,a} &= \partial_1 A_{3,a} - \partial_3 A_{1,a} = -a \left[A_0 \partial_x \tilde{M} - 2A_4 M_1 k_c^2 \partial_z u_{xz} \right].
\end{aligned} \tag{25}$$

With Eq. (15) and Eq(13) for Φ_a and $A_{\mu,a}^{pse}$, we can obtain the total effective action

$$S_{ax} = \int dt d^3r \left(\frac{1}{2A_0^2 M_1 k_c} \right) \frac{\theta}{2\pi^2} \left[\partial_x \tilde{C} \left(J \partial_z u_{yz} - A_0^2 \partial_y \tilde{M} \right) + \partial_y \tilde{C} \left(-J \partial_z u_{xz} + A_0^2 \partial_x \tilde{M} \right) + \partial_z \tilde{C} \left(-J \partial_x u_{yz} + J \partial_y u_{xz} \right) \right] \tag{26}$$

where $J = -2A_0 A_4 M_0$. One notices that all the terms that depend on time derivative contain the valley index a because of time reversal symmetry, so they vanish when summing over a . We can write S_{ax} as a sum of total derivatives as

$$S_{ax} = \int dt d^3r \left(\frac{1}{2A_0^2 M_1 k_c} \right) \frac{\theta}{2\pi^2} \left[\partial_x \left[\tilde{C} \left(J \partial_z u_{yz} - A_0^2 \partial_y \tilde{M} \right) \right] + \partial_y \left[\tilde{C} \left(-J \partial_z u_{xz} + A_0^2 \partial_x \tilde{M} \right) \right] + \partial_z \left[\tilde{C} \left(-J \partial_x u_{yz} + J \partial_y u_{xz} \right) \right] \right] \tag{27}$$

We assume periodic conditions along the x and z directions, as such being total derivatives, these contributions vanish.

We are left with the y dependence of θ and redefine $\frac{\theta}{2\pi^2} \left(\frac{1}{2A_0^2 M_1 k_c} \right) \rightarrow \theta$ so that the effective action is re-written as

$$S_{ax} = - \int dt dx dy dz \frac{\partial \theta}{\partial y} \left[\tilde{C} \left(-J \partial_z u_{xz} + A_0^2 \partial_x \tilde{M} \right) \right] \tag{28}$$

D. Symmetries of S_{ax}

The parameter θ in the effective action is originated from the valley axion field Φ_a , and therefore the symmetry properties of θ need not necessarily follow the symmetry properties of the standard axion term. In this section, we summarize the symmetries of the effective action S_{ax} as follows. Under six-fold rotation, C_{6z} , the effective action S_{ax} is invariant. Since the strain tensors as well as the partial derivatives are even under time-reversal, S_{ax} is invariant under time-reversal symmetry. Under inversion, the strain tensors are even whereas the partial derivatives are odd. But as can be seen in Eq(26), the partial derivatives occur in pairs. So S_{ax} is invariant under inversion as well. S_{ax} is also invariant under two-fold rotation C_{2x} and x -reflection m_x .

1. Six-fold rotation: \hat{C}_{6z}

Under C_{6z} , which is defined by the following transformation (for $\phi = 2\pi/6$)

$$\begin{pmatrix} x' \\ y' \\ z' \end{pmatrix} = \begin{pmatrix} \cos \phi & -\sin \phi & 0 \\ \sin \phi & \cos \phi & 0 \\ 0 & 0 & 1 \end{pmatrix} \begin{pmatrix} x \\ y \\ z \end{pmatrix}, \quad (29)$$

we have

$$\begin{aligned} \partial'_x &= \cos \phi \partial_x - \sin \phi \partial_y; \partial'_y = \sin \phi \partial_x + \cos \phi \partial_y; \partial'_z = \partial_z \\ u'_{xz} &= \cos \phi u_{xz} - \sin \phi u_{yz}; u'_{yz} = \sin \phi u_{xz} + \cos \phi u_{yz}; u'_{zz} = u_{zz} \\ u'_{xx} - u'_{yy} &= \cos 2\phi (u_{xx} - u_{yy}) - \sin 2\phi (2u_{xy}); 2u'_{xy} = \sin 2\phi (u_{xx} - u_{yy}) + \cos 2\phi (2u_{xy}) \\ u'_{xx} + u'_{yy} &= u_{xx} + u_{yy}; \tilde{C}' = \tilde{C}; \tilde{M}' = \tilde{M}. \end{aligned}$$

which lead to

$$\cot \theta' = \frac{u'_{xx} - u'_{yy}}{2u'_{xy}} = \frac{(u_{xx} - u_{yy}) \cot 2\phi - (2u_{xy})}{(u_{xx} - u_{yy}) + 2u_{xy} \cot 2\phi} = \cot (\theta + 2\pi/3) \quad (30)$$

and

$$\begin{aligned} &\partial'_x \tilde{C}' \left(J \partial'_z u'_{yz} - \partial'_y \tilde{M}' \right) + \partial'_y \tilde{C}' \left(-J \partial'_z u'_{xz} + \partial'_x \tilde{M}' \right) + \partial'_z \tilde{C}' \left(-J \partial'_x u'_{yz} + J \partial'_y u'_{xz} \right) \\ &= \left(\cos \phi \partial_x \tilde{C} - \sin \phi \partial_y \tilde{C} \right) \left(J \sin \phi \partial_z u_{xz} + J \cos \phi \partial_z u_{yz} - \sin \phi \partial_x \tilde{M} - \cos \phi \partial_y \tilde{M} \right) \\ &- \left(\sin \phi \partial_x \tilde{C} + \cos \phi \partial_y \tilde{C} \right) \left(J \cos \phi \partial_z u_{xz} - J \sin \phi \partial_z u_{yz} - \cos \phi \partial_x \tilde{M} + \sin \phi \partial_y \tilde{M} \right) \\ &- \partial_z \tilde{C} \left(J (\cos \phi \partial_x - \sin \phi \partial_y) (\sin \phi u_{xz} + \cos \phi u_{yz}) - J (\sin \phi \partial_x + \cos \phi \partial_y) (\cos \phi u_{xz} - \sin \phi u_{yz}) \right) \\ &= \partial_x \tilde{C} \left(J \partial_z u_{yz} - \partial_y \tilde{M} \right) + \partial_y \tilde{C} \left(-J \partial_z u_{xz} + \partial_x \tilde{M} \right) + \partial_z \tilde{C} \left(-J \partial_x u_{yz} + J \partial_y u_{xz} \right). \end{aligned} \quad (31)$$

Therefore, under C_{6z} , $\theta \rightarrow \theta + 2\pi/3$ i.e.

$$\begin{aligned} S'_{ax} &= \int dt d^3r \left(\frac{1}{2A_0^2 M_1 k_c} \right) \frac{\theta + 2\pi/3}{2\pi^2} \left[\partial_x \tilde{C} \left(J \partial_z u_{yz} - A_0^2 \partial_y \tilde{M} \right) + \partial_y \tilde{C} \left(-J \partial_z u_{xz} + A_0^2 \partial_x \tilde{M} \right) + \partial_z \tilde{C} \left(-J \partial_x u_{yz} + J \partial_y u_{xz} \right) \right] \\ &= \int dt d^3r \left(\frac{1}{2A_0^2 M_1 k_c} \right) \frac{\theta}{2\pi^2} \left[\partial_x \tilde{C} \left(J \partial_z u_{yz} - A_0^2 \partial_y \tilde{M} \right) + \partial_y \tilde{C} \left(-J \partial_z u_{xz} + A_0^2 \partial_x \tilde{M} \right) + \partial_z \tilde{C} \left(-J \partial_x u_{yz} + J \partial_y u_{xz} \right) \right] \\ &+ \int dt d^3r \left(\frac{1}{2A_0^2 M_1 k_c} \right) \frac{2\pi/3}{2\pi^2} \left[\partial_x \tilde{C} \left(J \partial_z u_{yz} - A_0^2 \partial_y \tilde{M} \right) + \partial_y \tilde{C} \left(-J \partial_z u_{xz} + A_0^2 \partial_x \tilde{M} \right) + \partial_z \tilde{C} \left(-J \partial_x u_{yz} + J \partial_y u_{xz} \right) \right] \\ &= S_{ax} \end{aligned} \quad (32)$$

In the second equality above, the second term is a total derivative and vanishes, thereby leaving S_{ax} invariant.

2. Two-fold rotation \hat{C}_{2x}

Under C_{2x} that transforms as

$$\begin{pmatrix} x' \\ y' \\ z' \end{pmatrix} = \begin{pmatrix} 1 & 0 & 0 \\ 0 & -1 & 0 \\ 0 & 0 & -1 \end{pmatrix} \begin{pmatrix} x \\ y \\ z \end{pmatrix} \quad (33)$$

we have

$$\begin{aligned} \partial'_x &= \partial_x; \partial'_{y,z} = -\partial_{y,z} \\ u'_{xz} &= -u_{xz}; u'_{yz} = u_{yz}; u'_{xx,yy,zz} = u_{xx,yy,zz} \\ 2u'_{xy} &= -2u_{xy}; u'_{xx} \pm u'_{yy} = u_{xx} \pm u_{yy} \\ \tilde{C}' &= \tilde{C}; \tilde{M}' = \tilde{M}, \end{aligned} \quad (34)$$

and

$$\cot \theta' = \frac{u'_{xx} - u'_{yy}}{2u'_{xy}} = -\frac{u_{xx} - u_{yy}}{2u_{xy}} = \cot(-\theta). \quad (35)$$

Since

$$\begin{aligned} &\partial'_x \tilde{C}' \left(J\partial'_z u'_{yz} - \partial'_y \tilde{M}' \right) + \partial'_y \tilde{C}' \left(-J\partial'_z u'_{xz} + \partial'_x \tilde{M}' \right) + \partial'_z \tilde{C}' \left(-J\partial'_x u'_{yz} + J\partial'_y u'_{xz} \right) \\ &= -\left[\partial_x \tilde{C} \left(J\partial_z u_{yz} - \partial_y \tilde{M} \right) + \partial_y \tilde{C} \left(-J\partial_z u_{xz} + \partial_x \tilde{M} \right) + \partial_z \tilde{C} \left(-J\partial_x u_{yz} + J\partial_y u_{xz} \right) \right], \end{aligned} \quad (36)$$

under C_{2x} , $S_{ax} \rightarrow S_{ax}$.

3. Reflection m_x

Under m_x that transforms as

$$\begin{pmatrix} x' \\ y' \\ z' \end{pmatrix} = \begin{pmatrix} -1 & 0 & 0 \\ 0 & 1 & 0 \\ 0 & 0 & 1 \end{pmatrix} \begin{pmatrix} x \\ y \\ z \end{pmatrix}, \quad (37)$$

we have

$$\begin{aligned} \partial'_x &= -\partial_x; \partial'_{y,z} = \partial_{y,z} \\ u'_{xz} &= -u_{xz}; u'_{yz} = u_{yz}; u'_{xx,yy,zz} = u_{xx,yy,zz} \\ 2u'_{xy} &= -2u_{xy}; u'_{xx} \pm u'_{yy} = u_{xx} \pm u_{yy} \\ \tilde{C}' &= \tilde{C}; \tilde{M}' = \tilde{M} \end{aligned} \quad (38)$$

and

$$\cot \theta' = \frac{u'_{xx} - u'_{yy}}{2u'_{xy}} = -\frac{u_{xx} - u_{yy}}{2u_{xy}} = \cot(-\theta). \quad (39)$$

Since

$$\begin{aligned} &\partial'_x \tilde{C}' \left(J\partial'_z u'_{yz} - \partial'_y \tilde{M}' \right) + \partial'_y \tilde{C}' \left(-J\partial'_z u'_{xz} + \partial'_x \tilde{M}' \right) + \partial'_z \tilde{C}' \left(-J\partial'_x u'_{yz} + J\partial'_y u'_{xz} \right) \\ &= -\left[\partial_x \tilde{C} \left(J\partial_z u_{yz} - \partial_y \tilde{M} \right) + \partial_y \tilde{C} \left(-J\partial_z u_{xz} + \partial_x \tilde{M} \right) + \partial_z \tilde{C} \left(-J\partial_x u_{yz} + J\partial_y u_{xz} \right) \right], \end{aligned} \quad (40)$$

under m_x , $S_{ax} \rightarrow S_{ax}$.

E. Bulk action

We first consider the bulk elastic wave in a hexagonal crystal lattice with D_{6h} symmetry group. The most general form of the elastic wave action is

$$S_0 = \int dt d^3r \left[\frac{1}{2} \rho_{ij} \partial_t u_i \partial_t u_j - F_0 \right]; \quad F_0 = \frac{1}{2} \lambda_{ijkl} u_{ij} u_{kl} \quad (41)$$

We assume the bulk to be uniform, i.e. $\rho_{ij} = \rho \delta_{ij}$ and denote the free energy as $F_0 = \frac{1}{2} \lambda_{ijkl} u_{ij} u_{kl}$. We follow Ref. [41] to construct the free energy for a hexagonal crystal by symmetry. We make a coordinate transformation, i.e. $\xi = x + iy, \eta = x - iy$. As a result, the n -fold rotation along the z -axis, \hat{C}_{nz} , gives $\hat{C}_{nz} \xi = \xi e^{i2\pi/n}, \hat{C}_{nz} \eta = \eta e^{-i2\pi/n}$. The derivatives transform as $\partial_\xi = \frac{1}{2} (\partial_x - i\partial_y), \partial_\eta = \frac{1}{2} (\partial_x + i\partial_y)$. The strain tensors transform as

$$\begin{aligned} u_{\xi\xi} &= u_{xx} - u_{yy} + 2iu_{xy}, u_{\eta\eta} = u_{xx} - u_{yy} - 2iu_{xy} \\ u_{\xi z} &= u_{xz} + iu_{yz}, u_{\eta z} = u_{xz} - iu_{yz}, u_{\xi\eta} = u_{xx} + u_{yy} \end{aligned} \quad (42)$$

We need F_0 to be constrained by the generators of the D_{6h} group. It turns out that the only constraint comes from the 6-fold rotation operator \hat{C}_{6z} . In order for F_0 to be invariant under \hat{C}_{6z} , the indices ξ and η must occur in pairs. For instance, a term of the form $\sim u_{\xi\xi} u_{\xi\eta}$ will break C_{6z} , which can be derived using Eq(42). Below, we write down all the possible terms and their combinatorial factors e.g. the term $\frac{1}{2} \lambda_{\xi\eta z z} u_{\xi\eta} u_{z z}$ would have a factor of 4 because $\lambda_{\xi\eta z z} = \lambda_{\eta\xi z z} = \lambda_{z z \eta\xi} = \lambda_{z z \xi\eta}$. The form of F_0 is

$$\begin{aligned} F_0 &= \frac{1}{2} \lambda_{z z z z} u_{z z}^2 + 4 \frac{1}{2} \lambda_{\xi\eta\xi\eta} u_{\xi\eta}^2 + 2 \frac{1}{2} \lambda_{\xi\xi\eta\eta} u_{\xi\xi} u_{\eta\eta} + 4 \frac{1}{2} \lambda_{\xi\eta z z} u_{\xi\eta} u_{z z} + 8 \frac{1}{2} \lambda_{\xi z \eta z} u_{\xi z} u_{\eta z} \\ &= \frac{1}{2} \lambda_{z z z z} u_{z z}^2 + 2 \lambda_{\xi\eta\xi\eta} u_{\xi\eta}^2 + \lambda_{\xi\xi\eta\eta} u_{\xi\xi} u_{\eta\eta} + 2 \lambda_{\xi\eta z z} u_{\xi\eta} u_{z z} + 4 \lambda_{\xi z \eta z} u_{\xi z} u_{\eta z} \end{aligned} \quad (43)$$

Using Eq(42), we transform the above free energy back into Cartesian coordinates and find

$$\begin{aligned} F_0 &= \frac{1}{2} \lambda_{z z z z} u_{z z}^2 + \frac{1}{2} \lambda_{x x x x} u_{x x}^2 + \frac{1}{2} \lambda_{y y y y} u_{y y}^2 + \lambda_{x x y y} u_{x x} u_{y y} + \lambda_{x x z z} u_{x x} u_{z z} \\ &\quad + \lambda_{y y z z} u_{y y} u_{z z} + 2 \lambda_{x y x y} u_{x y}^2 + 2 \lambda_{x z x z} u_{x z}^2 + 2 \lambda_{y z y z} u_{y z}^2 \end{aligned} \quad (44)$$

We define

$$\begin{aligned} \lambda_{x x x x} &= \lambda_{y y y y} = a + b, \lambda_{x x y y} = a - b, \lambda_{x y x y} = b, \lambda_{x x z z} = \lambda_{y y z z} = c \\ \lambda_{x z x z} &= \lambda_{y z y z} = d, \lambda_{z z z z} = f \end{aligned} \quad (45)$$

which correspond to

$$4 \lambda_{\xi\eta\xi\eta} = a, 2 \lambda_{\xi\xi\eta\eta} = b, 2 \lambda_{\xi\eta z z} = c, 2 \lambda_{\xi z \eta z} = d, \lambda_{z z z z} = f \quad (46)$$

For Na_3Bi , the elastic tensor [50, 51] can be written in a matrix form

$$\Lambda_{\text{theoretical}} = \begin{pmatrix} \lambda_{x x x x} & \lambda_{x x y y} & \lambda_{x x z z} & 0 & 0 & 0 \\ \lambda_{y y x x} & \lambda_{y y y y} & \lambda_{y y z z} & 0 & 0 & 0 \\ \lambda_{z z x x} & \lambda_{z z y y} & \lambda_{z z z z} & 0 & 0 & 0 \\ 0 & 0 & 0 & \lambda_{y z y z} & 0 & 0 \\ 0 & 0 & 0 & 0 & \lambda_{x z x z} & 0 \\ 0 & 0 & 0 & 0 & 0 & \lambda_{x y x y} \end{pmatrix} = \begin{pmatrix} a + b & a - b & c & 0 & 0 & 0 \\ a - b & a + b & c & 0 & 0 & 0 \\ c & c & f & 0 & 0 & 0 \\ 0 & 0 & 0 & d & 0 & 0 \\ 0 & 0 & 0 & 0 & d & 0 \\ 0 & 0 & 0 & 0 & 0 & b \end{pmatrix}, \quad (47)$$

The values of the paramters a, b, c, d, f can be found in Table S4 according to Refs. [50, 51].

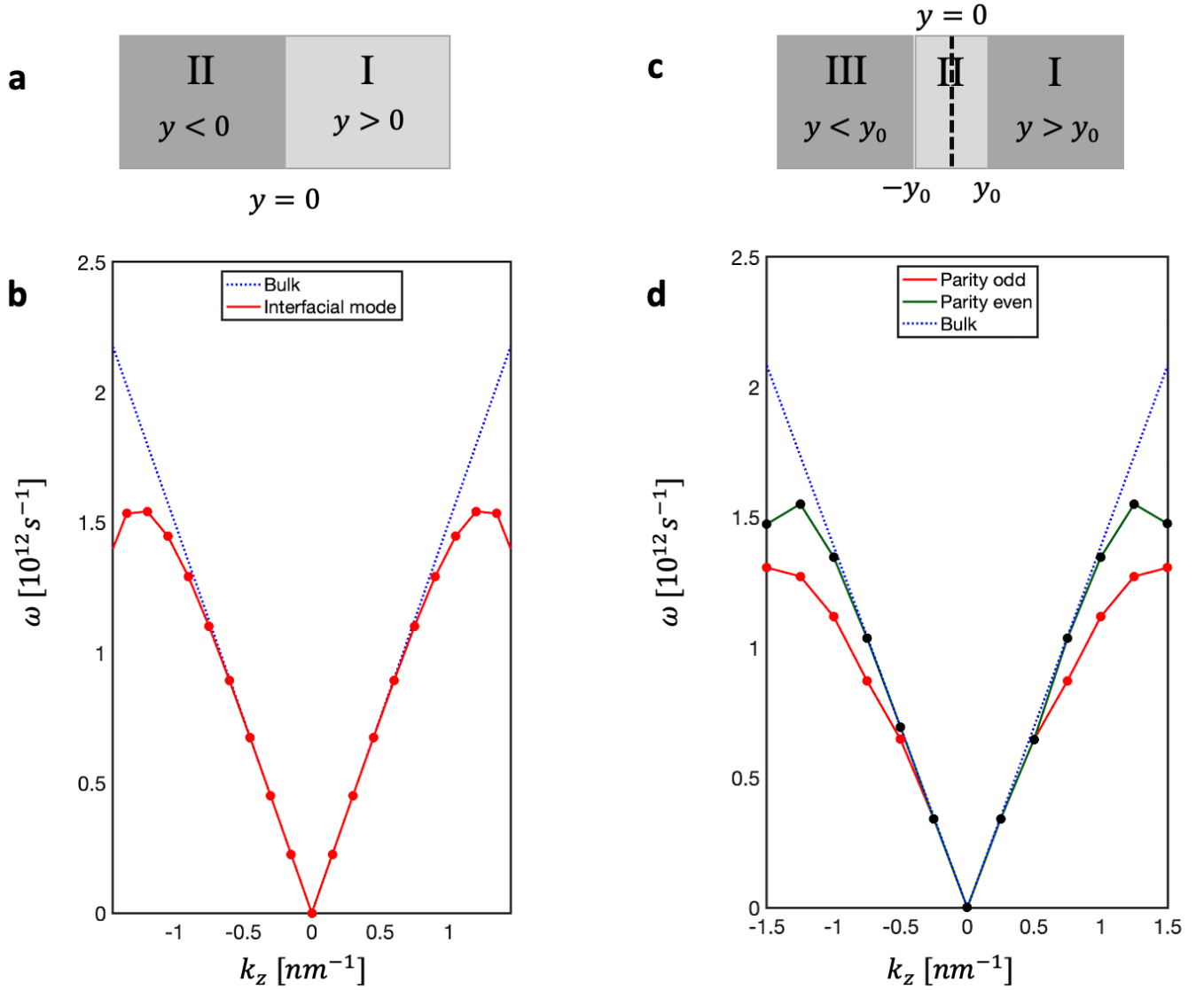


FIG. S3. (a) Regions I and II for *Case I* (b) Interfacial mode (red) frequency as a function of k_z (for $k_x = 0$) and $c_0 = 1.5 \times 10^3 m/s$, $r = 0.8$ in units of $10^{-12} m^4/s^2$ (c) Regions I, II and III for *Case II*. (d) Frequency of interfacial modes (even and odd parities) for $k_x = 0$ and $\frac{\theta_0 s}{y_0} = 5$ in units of $10^{-9} m^4/s^2$ with $a = 6.75, b = 3.17$ in units of $10^6 m^2/s^2$

F. Equation of motion with the Axion term

In this section, we derive the full equation of motion including the axion contribution. Here we rewrite the axion action S_{ax} into a general form $S_{ax} = S_{11} + S_{12} + S_{13}$ where (assuming Einstein's summation convention)

$$S_{11} = - \int d^3r \frac{\partial \theta}{\partial y} \left[\xi_{ijkl} \partial_k u_i \partial_l \partial_s u_j \right] \quad (48)$$

$$S_{12} = - \int d^3r \frac{\partial \theta}{\partial y} \left[\eta_{ijkl} \partial_k u_i \partial_y \partial_l u_j \right] \quad (49)$$

$$S_{13} = - \int d^3r \frac{\partial \theta}{\partial y} \left[\phi_{ijk} \partial_y u_i \partial_y \partial_k u_j \right]. \quad (50)$$

By expanding Eq(28), we find

$$\begin{aligned}
S_1 &= \int d^3r \frac{\partial\theta}{\partial y} \left[-\frac{J}{2}C_3\partial_z u_z \partial_z^2 u_x - \frac{J}{2}C_3\partial_z u_z \partial_x \partial_z u_z - \frac{J}{2}C_4\partial_x u_x \partial_z^2 u_x - \frac{J}{2}C_4\partial_x u_x \partial_x \partial_z u_z \right. \\
&\quad - \frac{J}{2}C_4\partial_y u_y \partial_z^2 u_x - \frac{J}{2}C_4\partial_y u_y \partial_x \partial_z u_z + A_0^2 M_3 C_3 \partial_z u_z \partial_x \partial_z u_z + A_0^2 C_4 M_3 \partial_x u_x \partial_x \partial_z u_z \\
&\quad + A_0^2 C_4 M_3 \partial_y u_y \partial_x \partial_z u_z + A_0^2 C_3 M_4 \partial_z u_z \partial_x^2 u_x + A_0^2 C_4 M_4 \partial_x u_x \partial_x^2 u_x + A_0^2 C_4 M_4 \partial_y u_y \partial_x^2 u_x \\
&\quad \left. + A_0^2 C_3 M_4 \partial_z u_z \partial_x \partial_y u_y + A_0^2 C_4 M_4 \partial_x u_x \partial_x \partial_y u_y + A_0^2 C_4 M_4 \partial_y u_y \partial_x \partial_y u_y \right] \\
&= \int d^3r \frac{\partial\theta}{\partial y} \left[-\frac{J}{2}C_3\partial_z u_z \partial_z^2 u_x - \frac{J}{2}C_4\partial_x u_x \partial_x \partial_z u_z - \frac{J}{2}C_4\partial_y u_y \partial_z^2 u_x - \frac{J}{2}C_4\partial_y u_y \partial_x \partial_z u_z \right. \\
&\quad \left. + A_0^2 C_4 M_3 \partial_x u_x \partial_x \partial_z u_z + A_0^2 C_4 M_3 \partial_y u_y \partial_x \partial_z u_z + A_0^2 C_3 M_4 \partial_z u_z \partial_x^2 u_x + A_0^2 C_3 M_4 \partial_z u_z \partial_x \partial_y u_y \right] \quad (51)
\end{aligned}$$

and thus we have the following expressions for ξ, η, ϕ (all other terms are zero)

$$\begin{aligned}
\xi_{zzzz} &= \frac{1}{4}C_3J; \xi_{zzzz} = -\frac{1}{4}C_3J \\
\xi_{zzxx} &= \xi_{zzxx} = \xi_{zzxx} = \frac{1}{6} \left(\frac{J}{2}C_4 + A_0^2 (C_3M_4 - C_4M_3) \right) \\
\xi_{zzxx} &= \xi_{zzxx} = \xi_{zzxx} = -\frac{1}{6} \left(\frac{J}{2}C_4 + A_0^2 (C_3M_4 - C_4M_3) \right) \\
\eta_{zyzy} &= \eta_{zyzy} = \eta_{zyzy} = \eta_{zyzy} = \eta_{zyzy} = \eta_{zyzy} = \frac{1}{12} \left(\frac{J}{2}C_4 + A_0^2 (C_3M_4 - C_4M_3) \right) \\
\eta_{yxzy} &= \eta_{yxzy} = \eta_{yxzy} = \eta_{yxzy} = \eta_{yxzy} = \eta_{yxzy} = -\frac{1}{12} \left(\frac{J}{2}C_4 + A_0^2 (C_3M_4 - C_4M_3) \right) \\
\eta_{xyzy} &= \eta_{xyzy} = \eta_{xyzy} = \frac{1}{6} \left(\frac{J}{2}C_4 \right) \\
\eta_{yxzy} &= \eta_{yxzy} = \eta_{yxzy} = -\frac{1}{6} \left(\frac{J}{2}C_4 \right) \quad (52)
\end{aligned}$$

We next hope to derive the contribution to the equation of motion from S_{ax} . We find

$$\begin{aligned}
\delta S_{11} &= - \int d^3r \frac{\partial\theta}{\partial y} \xi_{ijkl} (\partial_k \delta u_i \partial_l \delta u_j + \partial_k u_i \partial_l \delta u_j) \\
&= - \int d^3r \frac{\partial\theta}{\partial y} \xi_{ijkl} (-\partial_l \partial_k \delta u_j \delta u_i + \partial_l \delta u_k \partial_k u_i \delta u_j) \\
&= \int d^3r \frac{\partial\theta}{\partial y} (\xi_{ijkl} - \xi_{jikl}) \partial_k \partial_l \delta u_j \delta u_i \quad (53)
\end{aligned}$$

so that the contribution to the equation of motion from the first term is $\frac{\partial\theta}{\partial y} (\xi_{ijkl} - \xi_{jikl}) \partial_k \partial_l \delta u_j$. Similarly,

$$\begin{aligned}
\delta S_{12} &= - \int d^3r \frac{\partial\theta}{\partial y} \eta_{ijkl} (\partial_k \delta u_i \partial_y \partial_l u_j + \partial_k u_i \partial_y \partial_l \delta u_j) \\
&= \int d^3r \eta_{ijkl} \left(\frac{\partial\theta}{\partial y} \delta u_i \partial_k \partial_y \partial_l u_j - \partial_y \left(\frac{\partial\theta}{\partial y} \partial_l \partial_k u_i \right) \delta u_j \right) \\
&= \int d^3r \left(\eta_{ijkl} \frac{\partial\theta}{\partial y} \partial_k \partial_y \partial_l u_j - \eta_{jikl} \partial_y \left(\frac{\partial\theta}{\partial y} \partial_k \partial_l u_j \right) \right) \delta u_i \quad (54)
\end{aligned}$$

so that the contribution to the equation of motion from the second term is $\eta_{ijkl} \frac{\partial\theta}{\partial y} \partial_k \partial_y \partial_l u_j - \eta_{jikl} \partial_y \left(\frac{\partial\theta}{\partial y} \partial_k \partial_l u_j \right)$;

$$\begin{aligned}
\delta S_{13} &= - \int d^3r \frac{\partial\theta}{\partial y} \phi_{ijk} (\partial_y \delta u_i \partial_y \partial_k u_j + \partial_y u_i \partial_y \partial_k \delta u_j) \\
&= - \int d^3r \phi_{ijk} \left(-\partial_y \left(\frac{\partial\theta}{\partial y} \partial_y \partial_k u_j \right) \delta u_i + \partial_y \left(\frac{\partial\theta}{\partial y} \partial_y \partial_k u_i \right) \delta u_j \right) \\
&= \int d^3r (\phi_{ijk} - \phi_{jik}) \partial_y \left(\frac{\partial\theta}{\partial y} \partial_y \partial_k u_j \right) \delta u_i \quad (55)
\end{aligned}$$

so that the contribution to the equation of motion from the third term is $(\phi_{ijk} - \phi_{jik}) \partial_y \left(\frac{\partial \theta}{\partial y} \partial_y \partial_k u_j \right)$.

Therefore, the full equation of motion can be obtained from $\frac{\delta S}{\delta u_i} = 0$ with $S = S_0 + S_{ax}$ where S_0 is given in Eq(41) and S_{ax} is given by Eqs(48-50), which lead to

$$\begin{aligned} \rho \ddot{u}_i &= \partial_j (\lambda_{ijkl} \partial_k u_l) + \frac{\partial \theta}{\partial y} (\xi_{ijkl} - \xi_{jikl}) \partial_k \partial_l \partial_s u_j + \eta_{ijkl} \frac{\partial \theta}{\partial y} \partial_k \partial_y \partial_l u_j - \eta_{jikl} \partial_y \left(\frac{\partial \theta}{\partial y} \partial_k \partial_l u_j \right) \\ &+ (\phi_{ijk} - \phi_{jik}) \partial_y \left(\frac{\partial \theta}{\partial y} \partial_y \partial_k u_j \right). \end{aligned} \quad (56)$$

S2. ANALYTIC SOLUTION OF AXION DOMAIN WALL MODES

A. Bulk axion domain wall

We consider periodic boundary conditions along x and z directions and an axion domain at the origin along the y direction, so the form of the θ function is given by $\theta(y) = -\frac{\theta_0}{2\pi^2} \Theta(y)$ where $\Theta(y)$ is the Heaviside step function. We assume the solution to decay exponentially at infinity. We rewrite $\frac{\theta_0}{2\pi^2} \frac{J}{2} C_3 \equiv r$, $\frac{\theta_0}{2\pi^2} \frac{J}{2} C_4 \equiv s$ and $\frac{\theta_0}{2\pi^2} A_0^2 (C_3 M_4 - C_4 M_3) \equiv t$ and $\alpha(k_x, k_z) = r k_z^3 - (s + t) k_x^2 k_z$. We choose the ansatz $\mathbf{u}(\mathbf{r}, t) = \mathbf{f}(y) e^{i\mathbf{k}_{\parallel} \cdot \mathbf{r}_{\parallel}}$ with $\mathbf{r}_{\parallel} = (x, z)$ and $\mathbf{k}_{\parallel} = (k_x, k_z)$. Then, $H\mathbf{f} = \omega^2 \mathbf{f}$ where $H = H_0 + H_{ax}$ with

$$H_0 = \begin{pmatrix} (a+b)k_x^2 + dk_z^2 - b\partial_y^2 & -ik_x a \partial_y & (c+d)k_x k_z \\ -ik_x a \partial_y & bk_x^2 + dk_z^2 - (a+b)\partial_y^2 & -ik_z(c+d)\partial_y \\ (c+d)k_x k_z & -ik_z(c+d)\partial_y & fk_z^2 + dk_x^2 - d\partial_y^2 \end{pmatrix}, \quad (57)$$

and

$$H_{ax} = \begin{pmatrix} 0 & -\frac{s}{2} k_z^2 \{\partial_y, \delta(y)\} & -i\delta(y)\alpha \\ \frac{s}{2} k_z^2 \{\partial_y, \delta(y)\} & 0 & +\frac{1}{2}(s+t)k_x k_z \{\partial_y, \delta(y)\} \\ i\delta(y)\alpha & -\frac{1}{2}(s+t)k_x k_z \{\partial_y, \delta(y)\} & 0 \end{pmatrix}, \quad (58)$$

and the form of the eigenvector \mathbf{f} is defined in the main text. Below we will first discuss two simplified situations, in which analytical solutions for the domain wall modes can be obtained.

B. Case I: α term

In this section, we consider the isotropic approximation, where $a = c_t^2 - c_l^2$, $b = d = c_t^2$, $c = c_l^2 - 2c_t^2$, $f = c_l^2$, and further assume $c_t = c_l = c_0$, and $r \neq 0$, $s = t = 0$. Thus, $H_{ph} = H_0 + \delta(y)h_1$ with

$$H_0 = \begin{pmatrix} c_0^2 k^2 - c_0^2 \partial_y^2 & 0 & 0 \\ 0 & c_0^2 k^2 - c_0^2 \partial_y^2 & 0 \\ 0 & 0 & c_0^2 k^2 - c_0^2 \partial_y^2 \end{pmatrix}, \quad (59)$$

and

$$h_1 = \begin{pmatrix} 0 & 0 & -i\alpha(k_x, k_z) \\ 0 & 0 & 0 \\ i\alpha(k_x, k_z) & 0 & 0 \end{pmatrix}. \quad (60)$$

Due to the δ -function in front of h_1 , we have two regions I and II for $y > 0$ and $y < 0$, respectively, as shown in Fig. S3a, and choose the ansatz of exponentially localized phonon modes around $y = 0$ such that they vanish at infinity i.e.

$$\mathbf{u} = \begin{cases} \sum_{\tau=1}^3 A_{\tau} e^{-\lambda_{\tau} y} \mathbf{u}_0^{\tau}(y, \lambda_{\tau}) & y > 0 \\ \sum_{\tau=1}^3 B_{\tau} e^{\xi_{\tau} y} \mathbf{v}_0^{\tau}(y, \xi_{\tau}) & y < 0 \end{cases} \quad (61)$$

where \mathbf{u}_0^τ and \mathbf{v}_0^τ are eigenmodes given by $u_i^\tau(y) = e^{-\lambda_\tau y} \delta_{i\tau}$ and $v_i^\tau(y) = e^{\xi_\tau y} \delta_{i\tau}$ with $\lambda_\tau = \xi_\tau = \sqrt{k^2 - \omega^2/c_0^2} > 0$. By writing down the boundary conditions at $y = 0$, we obtain 6 equations for 6 coefficients $A_{1,2,3}$ and $B_{1,2,3}$ given by (for $i = x, y, z$)

$$\begin{aligned} \sum_{\tau=1}^3 u_i^\tau(0^+, \lambda_\tau) A_\tau - \sum_{\tau=1}^3 v_i^\tau(0^-, \xi_\tau) B_\tau &= 0 \\ \sum_{\tau=1}^3 \left[\sum_j (h_1)_{ij} u_j^\tau(0, \lambda_\tau) + c_0^2 \lambda_\tau u_i^a(0, \lambda_\tau) \right] A_\tau + \sum_{\tau=1}^3 \left[\sum_j (h_1)_{ij} v_j^\tau(0, \xi_\tau) + c_0^2 \xi_\tau v_i^a(0, \xi_\tau) \right] B_\tau &= 0 \end{aligned} \quad (62)$$

Eq(62) can be written in a compact form as

$$M_{6 \times 6} \begin{pmatrix} A \\ B \end{pmatrix} = 0, \quad (63)$$

where

$$M = \begin{pmatrix} \mathbb{I}_{3 \times 3} & -\mathbb{I}_{3 \times 3} \\ h_1 + c_0^2 \sqrt{k^2 - \omega^2/c_0^2} \mathbb{I}_{3 \times 3} & h_1 + c_0^2 \sqrt{k^2 - \omega^2/c_0^2} \mathbb{I}_{3 \times 3} \end{pmatrix} \quad (64)$$

and $A = (A_1, A_2, A_3)^T$ and $B = (B_1, B_2, B_3)^T$. A nontrivial solution exists if the secular equation ($\det(M) = 0$)

$$c_0^2 \sqrt{k^2 - \omega^2/c_0^2} \left(c_0^4 (k^2 - \omega^2/c_0^2)^2 - \alpha^2 \right) = 0 \quad (65)$$

is satisfied. Eq(65) has two solutions, $\omega = c_0 k$ is the bulk mode and $\omega = \left[(c_0 k)^2 - (\alpha(k_x, k_z)/c_0)^2 \right]^{1/2}$ is an interfacial mode with a dispersion with the energy lower than the bulk mode, as depicted by the red line in Fig. S3b. This gives $\lambda = |\alpha(k_x, k_z)|/c_0^2$. From Eq(63), we have $A_2 = B_2 = 0$, $A_1 = B_1$ and $A_3 = B_3$, which leads to

$$c_0^2 \lambda A_1 - i \alpha A_3 = 0 \implies A_1 = i \frac{\alpha}{c_0^2 \lambda} A_3 = i \frac{\alpha}{c_0^2 |\alpha|/c_0^2} A_3 = i \text{sgn}(\alpha) A_3. \quad (66)$$

The interfacial phonon displacement field has the eigenvector form

$$\mathbf{u} = N e^{-\lambda|y|} \begin{pmatrix} \text{sgn}(\alpha) \\ 0 \\ i \end{pmatrix} \quad (67)$$

with the normalization factor N . The above eigen-function of phonon modes is circularly polarized and the corresponding phonon angular momentum, defined by $l_i = \hbar \mathbf{u}_0^\dagger M_i \mathbf{u}_0$ where $i = x, y, z$ and $(M_i)_{jk} = (-i) \epsilon_{ijk}$ [52, 53], has non-zero component, $l_y = \text{sgn}(\alpha) \hbar$, which is fully circularly polarized with its helicity depending on the sign of α that in turn depends on the sign of k_z ($\alpha = r k_z^3$).

C. Case II: only $s \neq 0$

For *Case II*, we choose $s \neq 0$ and $r = s + t = 0$. We will show the existence of two interface modes in this limit, which explains Fig. 1d of the main text. Due to the presence of $\{\partial_y, \frac{\partial \theta}{\partial y}\}$ term, we cannot treat $\frac{\partial \theta}{\partial y}$ as $\delta(y)$ analytically. Instead, we consider a linear change in θ . We divide the system into three regions i.e. I ($y > y_0$), II ($-y_0 < y < y_0$) and III ($y < -y_0$) as shown in Fig. S3c, in which

$$\theta(y) = \begin{cases} -\theta_0 & y > y_0 \\ -\theta_0 \frac{y}{y_0} & -y_0 < y < y_0 \\ \theta_0 & y < -y_0 \end{cases} \quad (68)$$

The Hamiltonian is found to be block diagonal (when $c + d = 0$) with the u_z part decoupled from u_x and u_y . We thus focus on the Hamiltonian for u_x and u_y , which is given by

$$H_{ph} = \begin{pmatrix} dk_z^2 - b\partial_y^2 & \frac{s}{2}k_z^2\{\partial_y, \frac{\partial\theta}{\partial y}\} \\ -\frac{s}{2}k_z^2\{\partial_y, \frac{\partial\theta}{\partial y}\} & dk_z^2 - (a+b)\partial_y^2 \end{pmatrix}, \quad (69)$$

and consider the ansatz

$$\mathbf{u} = \begin{cases} \sum_{\alpha=1,2} A_{\alpha} e^{-\lambda_{\alpha} y} \chi_{\alpha}^I & \text{Region I} \\ \sum_{\alpha=1,2} B_{\alpha'} e^{ik_{\alpha'} y} \chi_{\alpha'}^{II} & \text{Region II} \\ \sum_{\alpha=1,2} C_{\alpha} e^{\lambda_{\alpha} y} \chi_{\alpha}^{III} & \text{Region III} \end{cases}. \quad (70)$$

The phonon Hamiltonian for three regions becomes (for $k_x = 0$)

$$H_I = H_{III} = \begin{pmatrix} dk_z^2 - b\lambda^2 & 0 \\ 0 & dk_z^2 - (a+b)\lambda^2 \end{pmatrix}, \quad (71)$$

$$H_{II} = \begin{pmatrix} dk_z^2 + bk^2 & -i\tilde{\theta}k \\ i\tilde{\theta}k & dk_z^2 + (a+b)k^2 \end{pmatrix}, \quad (72)$$

where

$$\tilde{\theta} = \frac{\theta_0 s}{y_0} k_z^2, \quad \lambda_1 = \sqrt{\frac{1}{b}(dk_z^2 - \omega^2)}, \quad \lambda_2 = \sqrt{\frac{1}{a+b}(dk_z^2 - \omega^2)}; \quad \chi_1^I = \begin{pmatrix} 1 \\ 0 \end{pmatrix}, \quad \chi_2^I = \begin{pmatrix} 0 \\ 1 \end{pmatrix} \quad (73)$$

and

$$k_1 = -\frac{1}{\sqrt{2b(a+b)}} \sqrt{(a+2b)(\omega^2 - dk_z^2) + \tilde{\theta}^2 - \sqrt{a^2(\omega^2 - dk_z^2)^2 + 2(a+2b)(\omega^2 - dk_z^2)\tilde{\theta}^2 + \tilde{\theta}^4}} \quad (74)$$

$$k_2 = -\frac{1}{\sqrt{2b(a+b)}} \sqrt{(a+2b)(\omega^2 - dk_z^2) + \tilde{\theta}^2 + \sqrt{a^2(\omega^2 - dk_z^2)^2 + 2(a+2b)(\omega^2 - dk_z^2)\tilde{\theta}^2 + \tilde{\theta}^4}} \quad (75)$$

$$\chi_1^{II} = \begin{pmatrix} i \left(ak^2 - \sqrt{a^2k^4 + 4k^2\tilde{\theta}^2} \right) \\ 2k\tilde{\theta} \end{pmatrix}, \quad \chi_2^{II} = \begin{pmatrix} i \left(ak^2 + \sqrt{a^2k^4 + 4k^2\tilde{\theta}^2} \right) \\ 2k\tilde{\theta} \end{pmatrix} \quad (76)$$

Since k has to be real, the expression inside the square root must be positive $a^2(\omega^2 - dk_z^2)^2 + 2(a+2b)(\omega^2 - dk_z^2)\tilde{\theta}^2 + \tilde{\theta}^4 > 0$ i.e. $\omega^2 > dk_z^2 - \frac{\tilde{\theta}^2}{a+2b+2\sqrt{(a+b)b}}$. For the θ configuration that is anti-symmetric with respect to $y = 0$, both the Hamiltonian H_0 and H_{ax} in Eqs(57,58) preserve mirror symmetry m_y and thus all eigenstates should also be the eigenstates of the m_y operator. We thus have two modes, corresponding to even and odd eigenvalues of the m_y operator i.e. $m_y \mathbf{u}(y) = \eta \mathbf{u}(-y)$ with $\eta = \pm$ where m_y is defined by $m_y \begin{pmatrix} u_x \\ u_y \end{pmatrix} = \begin{pmatrix} 1 & 0 \\ 0 & -1 \end{pmatrix} \begin{pmatrix} u_x \\ u_y \end{pmatrix}$. Due to the \hat{m}_y symmetry, we only need to focus on the interface at $y = y_0$ between Regions I and II. As

$$\mathbf{u}_{II} = \begin{cases} \sum_{\alpha=1}^2 \begin{pmatrix} B_{\alpha+} \cos(k_{\alpha} y) (ak_{\alpha}^2 - m(k_{\alpha})) \\ B_{\alpha+} \sin(k_{\alpha} y) (2k_{\alpha} \tilde{\theta}) \end{pmatrix}, & \eta = + \\ \sum_{\alpha=1}^2 \begin{pmatrix} -B_{\alpha+} \sin(k_{\alpha} y) (ak_{\alpha}^2 - m(k_{\alpha})) \\ B_{\alpha+} \cos(k_{\alpha} y) (2k_{\alpha} \tilde{\theta}) \end{pmatrix}, & \eta = - \end{cases} \quad (77)$$

where $m(k_{\alpha}) = \sqrt{a^2k_{\alpha}^2 + 4k_{\alpha}^2\tilde{\theta}^2}$, similar to *Case I*, the boundary conditions are given by

$$u_I(y = y_0) = u_{II}^{\eta=\pm}(y = y_0) \quad (78)$$

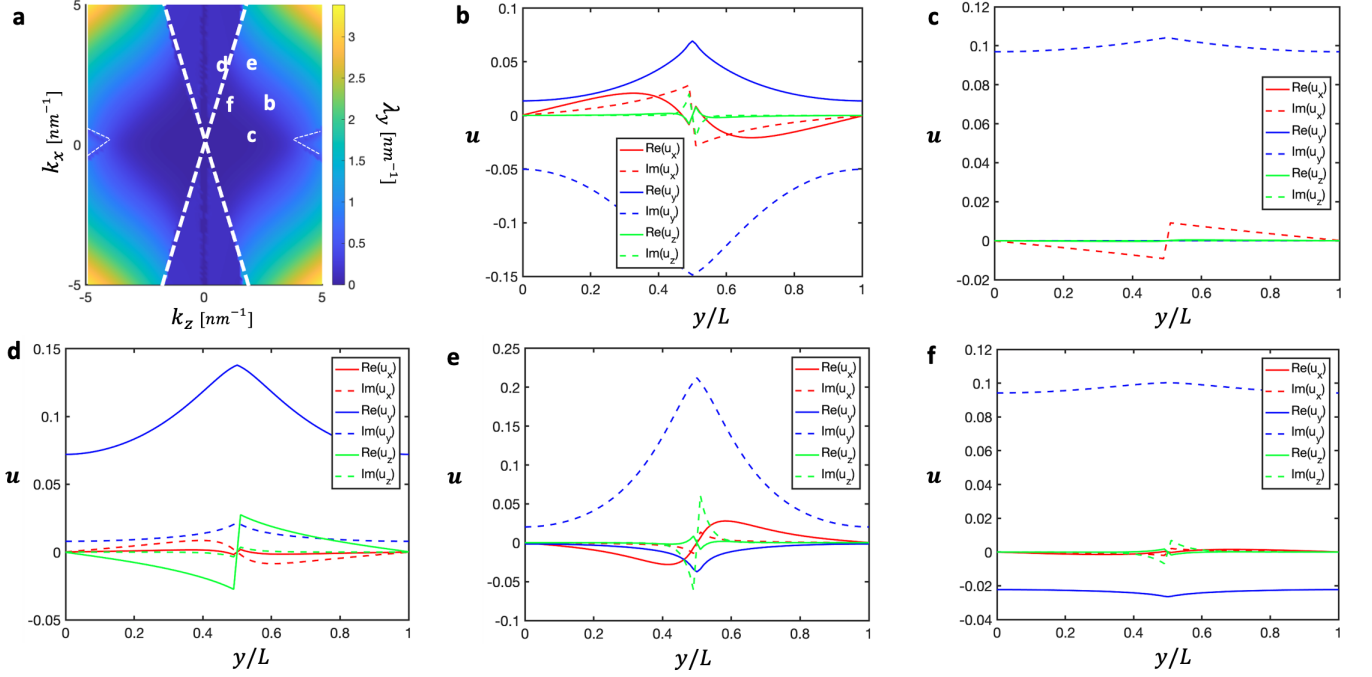


FIG. S4. (a) The inverse localization length λ_y as a function of (k_x, k_z) and the spatial distribution of the real and imaginary parts of the displacement field of the interface phonon mode for $(k_x, k_z; \lambda_y) =$ (b) (1,3;0.30) (c) (0,2;0.02) (d) (2.5,1;0.14) (e) (2.5,2;0.51) (f) (1,1;0.02) [in nm^{-1}]. We use $r = .8$; $s = .713$; $t = .9$ in units of $10^{-12} \text{m}^4/\text{s}^2$ and $a = 6.75, b = 3.17, c = 1.01, d = 1.93, f = 11.02$ in units of $10^6 \text{m}^2/\text{s}^2$.

$$v_y^I u_I(y = y_0) = v_y^{II} u_{II}^{\eta=\pm}(y = y_0) \quad (79)$$

$$\begin{pmatrix} -2ib\partial_y & \\ & -2i(a+b)\partial_y \end{pmatrix} \mathbf{u}_I(y = y_0) = \begin{pmatrix} -2ib\partial_y & -i\tilde{\theta} \\ i\tilde{\theta} & -2i(a+b)\partial_y \end{pmatrix} \mathbf{u}_{II}^{\eta=\pm}(y = y_0) \quad (80)$$

where $v_y^{I,II} = \frac{\partial H_{I,II}}{\partial k_y}$ is the velocity operator. Similar to *Case I*, we rewrite the above as

$$G_{4 \times 4}^{\eta=\pm} \begin{pmatrix} A \\ B \end{pmatrix} = 0 \quad (81)$$

where $A = (A_1, A_2)^T$ and $B = (B_{1,+}, B_{2,+})^T$. Explicitly,

$$G^+ = \begin{pmatrix} 1 & 0 & -\cos(k_1 y_0) g_1 & -\cos(k_2 y_0) g_2 \\ 0 & 1 & -\sin(k_1 y_0) (2k_1 \tilde{\theta}) & -\sin(k_2 y_0) (2k_2 \tilde{\theta}) \\ b\lambda_1 & 0 & k_1 \sin(k_1 y_0) (\tilde{\theta}^2 - bg_1) & k_2 \sin(k_2 y_0) (\tilde{\theta}^2 - bg_2) \\ 0 & (a+b)\lambda_2 & \tilde{\theta} \cos(k_1 y_0) (2(a+b)k_1^2 - g_1/2) & \tilde{\theta} \cos(k_2 y_0) (2(a+b)k_2^2 - g_2/2) \end{pmatrix} \quad (82)$$

and

$$G^- = \begin{pmatrix} 1 & 0 & \sin(k_1 y_0) g_1 & \sin(k_2 y_0) g_2 \\ 0 & 1 & -\cos(k_1 y_0) (2k_1 \tilde{\theta}) & -\cos(k_2 y_0) (2k_2 \tilde{\theta}) \\ b\lambda_1 & 0 & k_1 \cos(k_1 y_0) (\tilde{\theta}^2 - bg_1) & k_2 \cos(k_2 y_0) (\tilde{\theta}^2 - bg_2) \\ 0 & (a+b)\lambda_2 & -\tilde{\theta} \sin(k_1 y_0) (2(a+b)k_1^2 - g_1/2) & -\tilde{\theta} \sin(k_2 y_0) (2(a+b)k_2^2 - g_2/2) \end{pmatrix} \quad (83)$$

where $g_i = ak_i^2 - \sqrt{a^2 k_i^4 + 4\tilde{\theta}^2 k_i^2}$ for $i = 1, 2$. We solve the secular equation $\det(G^\pm) = 0$ numerically and find the dispersion of two interface modes, depicted by the red and dark green lines in Fig. S3d.

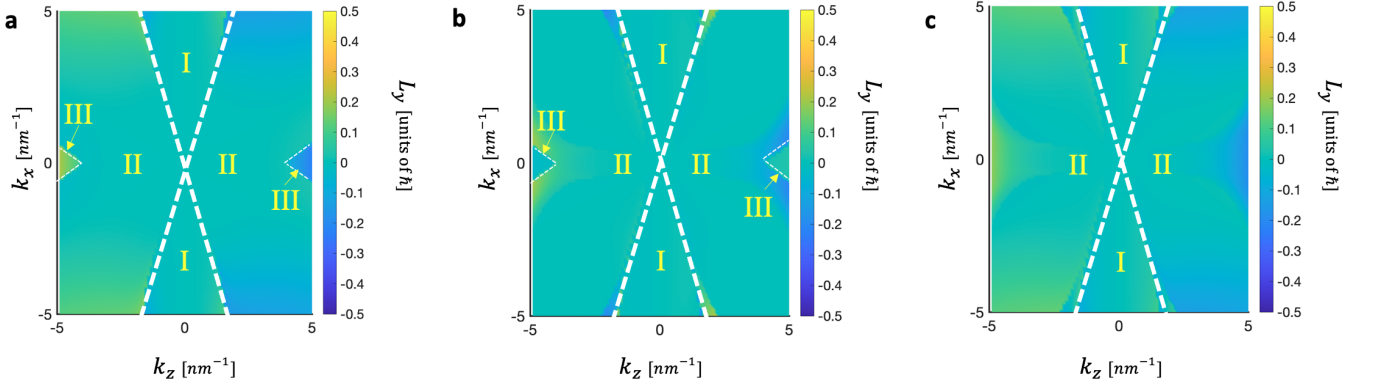


FIG. S5. (a) The out of plane (y component) phonon angular momentum of the lowest mode as a function of (k_x, k_z) (b) The out of plane (y component) phonon angular momentum of the second lowest mode as a function of (k_x, k_z) (c) The out of plane (y component) phonon angular momentum of the lowest two modes added together as a function of (k_x, k_z) . We use $r = .8$; $s = .713$; $t = .9$ in units of $10^{-12}m^4/s^2$ and $a = 6.75, b = 3.17, c = 1.01, d = 1.93, f = 11.02$ in units of $10^6m^2/s^2$

S3. NUMERICAL METHOD

In this section, we outline the numerical methods for solving the lattice model version of Eigen-equation (4) in the main text with an axion domain wall perpendicular to the $x - z$ plane. We consider a lattice regularization along y by dividing the y axis into $N + 1$ discrete sites with periodic boundaries at $i = 1$ and $i = N + 1$.

A. H_0 term

We define the components of \vec{u} as $u_i^x = \varphi_{3i-2}, u_i^y = \varphi_{3i-1}, u_i^z = \varphi_{3i}$ where $i = 1, 2, \dots, N + 1$. We start with $-\rho\omega^2 u_i = \partial_j(\lambda_{ijkl}\partial_k u_l)$ and define $L_{in,lm}$ such that $-\rho\omega^2 u_i(y_n) = L_{in,lm} u_l(y_m)$ with $L = L^{(0)} + L^{(1)} + L^{(2)}$. Here, $u_l(y_m) = \varphi_{3(m-1)+l}$

$$\begin{aligned}
L_{in,lm}^{(0)} &= -k_j k_k \lambda_{ijkl} \delta_{mn} \\
L_{in,ln+1}^{(1)} &= \frac{ik_k}{2\hbar} (\lambda_{iykl}(y_{n+1}) + \lambda_{lyki}(y_n)) \\
L_{ln+1,in}^{(1)} &= L_{in,ln+1}^{(1)*} \\
L_{in,ln+1}^{(2)} &= \frac{1}{2\hbar^2} (\lambda_{iyyi}(y_{n+1}) + \lambda_{iyyi}(y_n)) \\
L_{ln+1,in}^{(2)} &= L_{in,ln+1}^{(2)*} \\
L_{in,ln}^{(2)} &= -\frac{1}{2\hbar^2} (\lambda_{iyyi}(y_{n+1}) + \lambda_{iyyi}(y_{n-1}) + 2\lambda_{iyyi}(y_n))
\end{aligned} \tag{84}$$

B. H_1 term

In the presence of the axion term, the total Hamiltonian is $H = H_0 + H_1$. Using Eqs(53,54, 55), we define the following operators using Einstein's summation convention

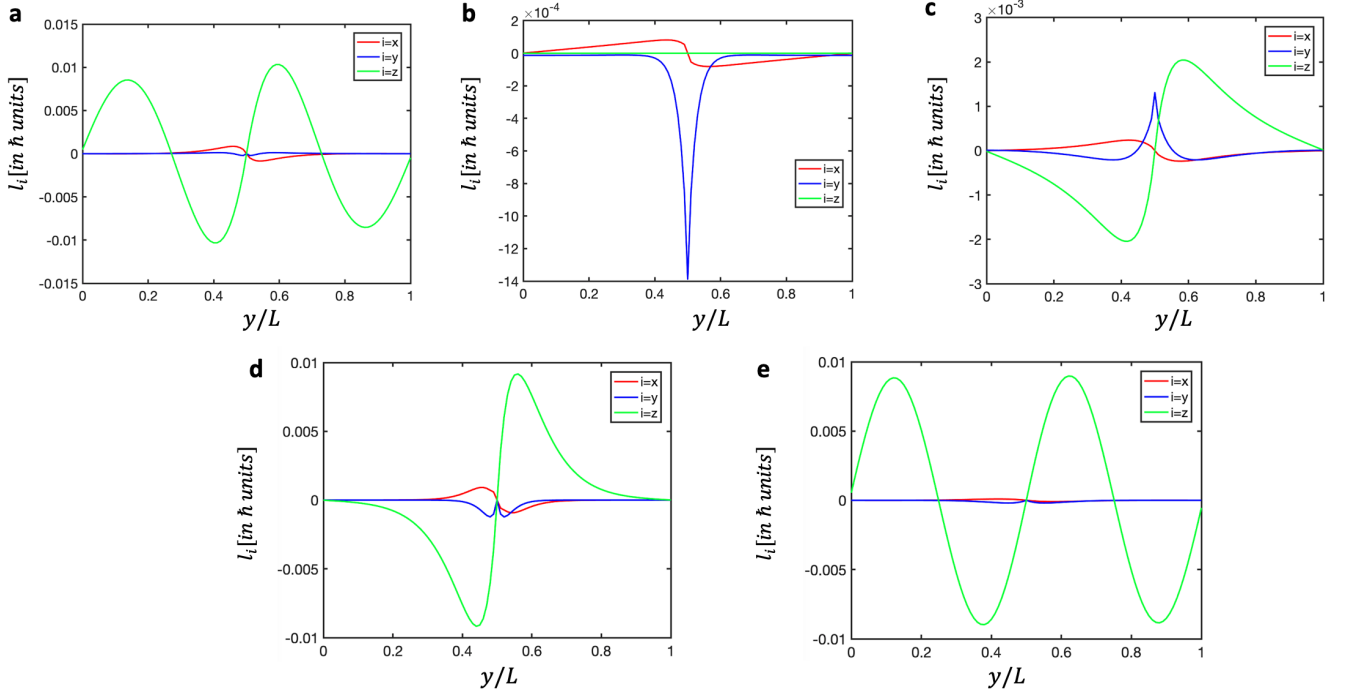


FIG. S6. The spatial distribution of phonon angular momentum of the interface phonon modes at $(k_x, k_z) =$ (a) (1,3) (b) (0,2) (c) (2.5,1) (d) (2.5,2) (e) (1,1) [in nm^{-1}]. We use $r = .8$; $s = .713$; $t = .9$ in units of $10^{-12}m^4/s^2$ and $a = 6.75, b = 3.17, c = 1.01, d = 1.93, f = 11.02$ in units of $10^6m^2/s^2$

$$\begin{aligned}
[L_{11}]_{in,jm} &= i \frac{\partial \theta}{\partial y}(y_m) (\xi_{ijkl} - \xi_{jikl}) k_k k_l k_s \delta_{nm} \\
[L_{12}]_{in,jn+1} &= \left(\eta_{ijkl} \frac{\partial \theta}{\partial y}(y_n) - \eta_{jikl} \frac{\partial \theta}{\partial y}(y_{n+1}) \right) \frac{k_k k_l}{2h} \\
[L_{12}]_{jn+1,in} &= [L_{11}]_{in,jn+1}^* \\
[L_{13}]_{in,jn+1} &= -\frac{ik_k}{2h^2} (\phi_{ijk} - \phi_{jik}) \left(\frac{\partial \theta}{\partial y}(y_n) + \frac{\partial \theta}{\partial y}(y_{n+1}) \right) \\
[L_{13}]_{jn+1,in} &= [L_{11}]_{in,jn+1}^* \\
[L_{13}]_{in,jn} &= \frac{ik_k}{2h^2} (\phi_{ijk} - \phi_{jik}) \left(\frac{\partial \theta}{\partial y}(y_{n+1}) + \frac{\partial \theta}{\partial y}(y_{n-1}) + 2 \frac{\partial \theta}{\partial y}(y_n) \right)
\end{aligned} \tag{85}$$

We consider the following axion domain wall (the discrete version for the step function)

$$\frac{\partial \theta}{\partial y}(y_n) = \begin{cases} -\theta_0/h, & \text{if } n = N/2. \\ 0, & \text{otherwise.} \end{cases} \tag{86}$$

C. Numerical Results

Here we will discuss our numerical results in Fig. S4-S7, to support our discussion of the interfacial modes in the main text. Fig. S4 shows the spatial profile of the real and imaginary parts of the displacement field for the interface phonon modes at five different momenta, which all reveal exponentially decaying behaviors away from the axion domain wall located at $y = L/2$. For small $|\mathbf{k}_{\parallel}|$, the spatial distribution is uniform, but gets more localized with increasing $|\mathbf{k}_{\parallel}|$.

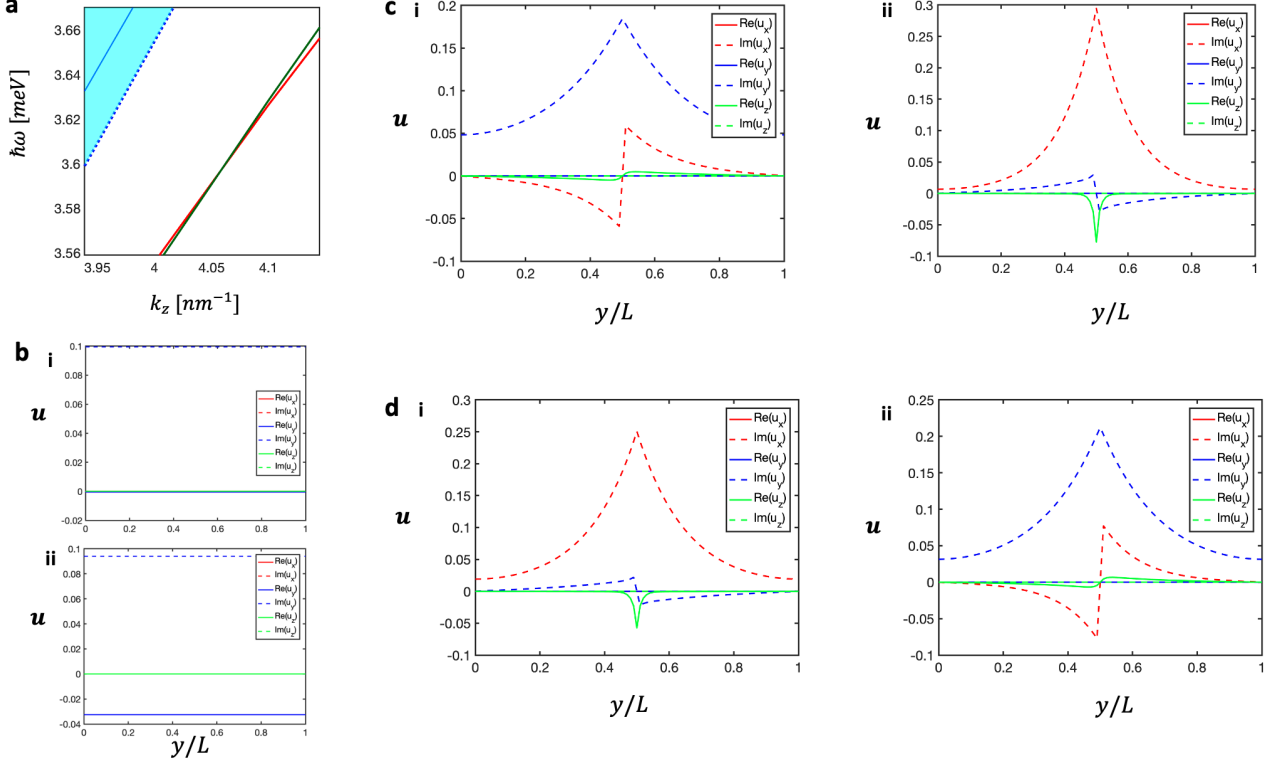


FIG. S7. (a) Band crossing between two interface phonon modes at around $k_z = 4.05 \text{ nm}^{-1}$ and $k_x = 0$. This is also the inset in Fig. 1d of the main text. (b) The spatial distribution of the real and imaginary parts of the displacement field of the lowest bulk phonon mode at (i) $k_z = 3.9 \text{ nm}^{-1}$ and (ii) $k_z = 4.2 \text{ nm}^{-1}$ (c) The spatial distribution of the real and imaginary parts of the displacement field of the lowest interface phonon mode at (i) $k_z = 3.9 \text{ nm}^{-1}$ and (ii) $k_z = 4.2 \text{ nm}^{-1}$ (d) The spatial distribution of the real and imaginary parts of the displacement field of the second lowest interface phonon mode at (i) $k_z = 3.9 \text{ nm}^{-1}$ and (ii) $k_z = 4.2 \text{ nm}^{-1}$

Fig. S5 and Fig. S6 provide information of the angular momentum of interfacial model modes. We find the interfacial phonon mode has a nonzero angular momentum component along the y direction l_y , and thus we show l_y as a function of \mathbf{k}_{\parallel} in Fig. S5. For most of \mathbf{k}_{\parallel} plane, the dominant phonon angular momentum comes from the lowest energy phonon mode (Fig. S5a), whereas the phonon angular momentum of the second lowest energy phonon mode is vanishingly small (Fig. S5b). However, we notice a rapid change of the phonon angular momenta for both the lowest and second lowest modes between the Region II and Region III, which is due to the crossing in energy between these two low energy phonon modes. The band crossing between the two interfacial modes is shown in Fig. S7a which occurs around $k_z = 4.05 \text{ nm}^{-1}$ and $k_x = 0$. The spatial distribution of the real and imaginary parts of the displacement field of the two interfacial modes is shown in Fig. S7c,d to conclusively identify their band crossing. The lowest bulk mode S7b shows no change. We also plot the spatial variation of l_i with $i = x, y, z$ as a function of y for various values of \mathbf{k}_{\parallel} in Fig. S6. The l_x and l_z components of the phonon angular momentum are anti-symmetric with respect to the axion domain wall at $y = L/2$, whereas the l_y component is symmetric. Thus, l_x and l_z vanish after summing over the y -locations, while l_y is still non-zero. Further, as \mathbf{k}_{\parallel} increases, the magnitude of $\sum_y l_y(y)$ increases.

S4. SURFACE PHONON MODES

We have discussed the existence of interface phonon modes. It is well known that surface acoustic wave can exist in an elastic material [41, 62]. In this section, we will study the influence of the axion term on the surface acoustic wave.

A. xz plane configuration

We consider a thin film model with the top ($y = y_1$) and bottom ($y = y_2$) surfaces parallel to the $x - z$ plane. In the absence of the axion term, the equation of motion is given by

$$\rho \ddot{u}_i = \partial_j \sigma_{ij} = \partial_j \frac{\partial F_0}{\partial u_{ij}} = \partial_j (\lambda_{ijkl} \partial_k u_l) \quad (87)$$

The elastic waves vanish at the bottom surface ($y = y_1$) and the top surface ($y = y_2$) is considered a stress free surface i.e. $u_x(y = y_1) = u_y(y = y_1) = u_z(y = y_1) = 0$ and $\sigma_{xy}(y = y_2) = \sigma_{yz}(y = y_2) = \sigma_{yy}(y = y_2) = 0$ where the stress tensors are

$$\sigma_{xy} = \frac{\partial F}{\partial u_{xy}} = 2b u_{xy} \quad (88)$$

$$\sigma_{yz} = \frac{\partial F}{\partial u_{yz}} = 2d u_{yz} \quad (89)$$

$$\sigma_{yy} = \frac{\partial F}{\partial u_{yy}} = (a + b) u_{yy} + (a - b) u_{xx} + c u_{zz} \quad (90)$$

It is possible to grow the sample on a substrate such that the top surface obeys free boundary condition whereas the bottom surface obeys open boundary conditions when the substrate density is much greater than the sample density. We impose periodic boundary conditions along x and z directions. We consider the wave ansatz of the form $u_i = f_i(y) e^{i(k_x x + k_z z - \omega t)}$. Therefore, k_x and k_z are good quantum numbers so that we can replace $\partial_x \rightarrow i k_x$ and $\partial_z \rightarrow i k_z$. After acting on the Ansatz, we simplify the equation of motion to the form $H_0 \mathbf{f} = \rho \omega^2 \mathbf{f}$ where

$$H_0 = \begin{pmatrix} (a+b)k_x^2 + dk_z^2 - b\partial_y^2 - (\partial_y b)\partial_y & -ik_x(a\partial_y + (\partial_y b)) & (c+d)k_x k_z \\ -ik_x(a\partial_y + (\partial_y b)) & bk_x^2 + dk_z^2 - (a+b)\partial_y^2 - \partial_y(a+b)\partial_y & -ik_z((c+d)\partial_y + (\partial_y c))\partial_y \\ (c+d)k_x k_z & -ik_z((c+d)\partial_y + (\partial_y c))\partial_y & fk_z^2 + dk_x^2 - d\partial_y^2 - (\partial_y d)\partial_y \end{pmatrix} \quad (91)$$

We denote the effective action for the axion term to be of the form

$$S_{ax} = - \int d^3 r \frac{\partial \theta(y)}{\partial y} \left[\xi_{ijkl} \partial_k u_i \partial_l \partial_s u_j + \eta_{ijkl} \partial_k u_i \partial_y \partial_l u_j + \phi_{ijk} \partial_y u_i \partial_y \partial_k u_j \right] \quad (92)$$

with $i, j = x, y, z$, $k, l, s = x, z$ and ξ, η, ϕ are given in Eq(52). Specifically, the axion contribution for the above thin film model is given by Eq(51),

$$S_{ax} = \int d^3 r \frac{\partial \theta}{\partial y} \left[-\frac{J}{2} C_3 \partial_z u_z \partial_x^2 u_x - \frac{J}{2} C_4 \partial_x u_x \partial_x \partial_z u_z - \frac{J}{2} C_4 \partial_y u_y \partial_z^2 u_x - \frac{J}{2} C_4 \partial_y u_y \partial_x \partial_z u_z \right. \\ \left. + A_0^2 C_4 M_3 \partial_x u_x \partial_x \partial_z u_z + A_0^2 C_4 M_3 \partial_y u_y \partial_x \partial_z u_z + A_0^2 C_3 M_4 \partial_z u_z \partial_x^2 u_x + A_0^2 C_3 M_4 \partial_z u_z \partial_x \partial_y u_y \right]. \quad (93)$$

The equation of motion is given by Eq(56) and Eq(52) i.e. $H \vec{f} = \rho \omega^2 \vec{f}$, where $H = H_0 + H_1$ with $H_1 = -(\partial_y \theta h_1 + \frac{1}{2} \partial_y^2 \theta h_2)$. We have used the redefined parameters r, s, t, α from Sec. S2 A,

$$h_1 = \begin{pmatrix} 0 & -s k_z^2 \partial_y & -i\alpha \\ s k_z^2 \partial_y & 0 & (s+t) k_x k_z \partial_y \\ i\alpha & -(s+t) k_x k_z \partial_y & 0 \end{pmatrix}, \quad h_2 = \begin{pmatrix} 0 & -s k_z^2 & 0 \\ s k_z^2 & 0 & (s+t) k_x k_z \\ 0 & -(s+t) k_x k_z & 0 \end{pmatrix} \quad (94)$$

B. Isotropic approximation for the bulk action without the Axion term

The isotropic free energy is given by

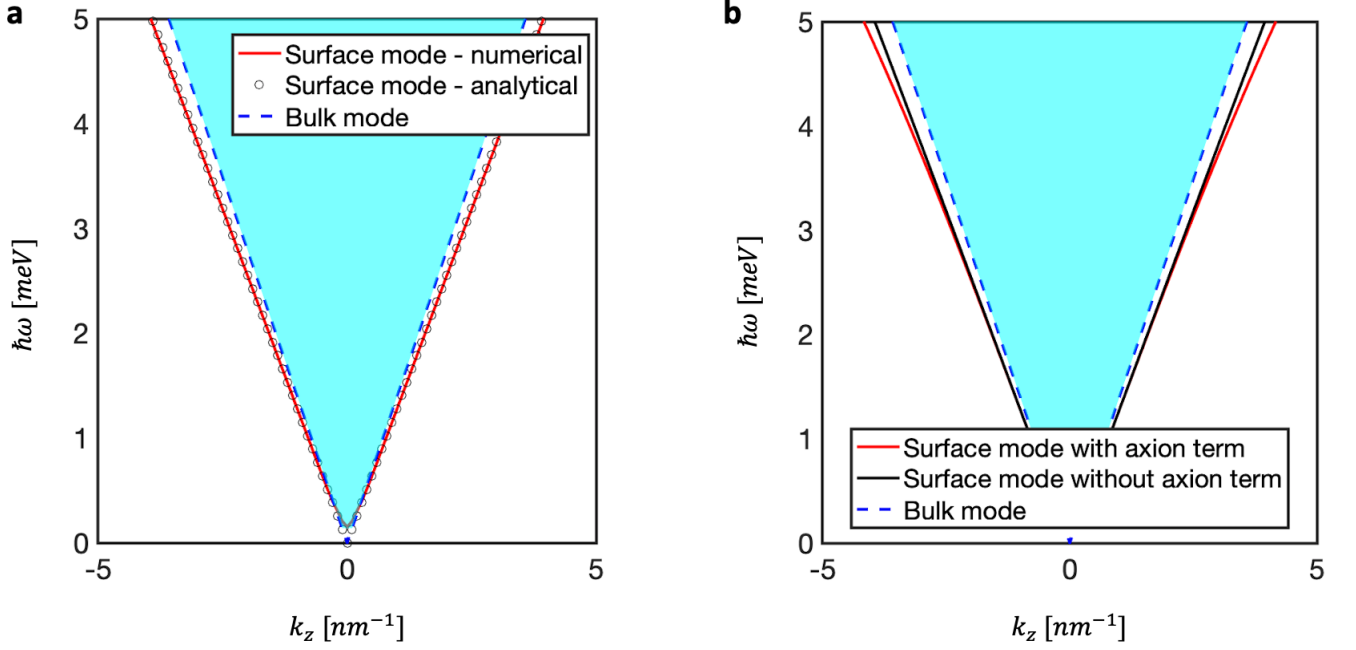


FIG. S8. (a) The existence of a surface phonon mode even in the absence of the axion term is shown, where the numerical result is depicted by the solid red line and the analytical result is depicted by black circles. (b) In the presence of the axion term, the energy of surface modes is lowered and is no longer linear in \mathbf{k} . We use $r = .8$; $s = .713$; $t = .9$ in units of $10^{-12}m^4/s^2$. For both the plots we consider the $k_x = k_z$ line and the isotropic approximation with $c_t = 1.5$ and $c_l = 1.5$ in units of $10^6m^2/s^2$.

$$F = \frac{\rho}{2} (c_l^2 - 2c_t^2) u_{ii}^2 + \rho c_t^2 u_{ik}^2 \quad (95)$$

The hexagonal crystal free energy given in Eq(45) boils down to the above isotropic limit when $a = \rho (c_l^2 - c_t^2)$, $b = d = \rho c_t^2$, $c = \rho (c_l^2 - 2c_t^2)$, $f = \rho c_l^2$. The equation of motion is thus:

$$\ddot{\mathbf{u}} = c_t^2 \nabla^2 \mathbf{u} + (c_l^2 - c_t^2) \nabla (\nabla \cdot \mathbf{u}) \quad (96)$$

Substituting the elastic wave ansatz form into Eq. (96), we have the eigen equation $H_0 \mathbf{f} = \omega^2 \mathbf{f}$ with

$$H_0 = \begin{pmatrix} c_l^2 k_x^2 + c_t^2 k_z^2 - c_t^2 \partial_y^2 - (\partial_y c_t^2) \partial_y & -ik_x (c_l^2 - c_t^2 + (\partial_y c_t^2)) \partial_y & k_x k_z (c_l^2 - c_t^2) \\ -ik_x (c_l^2 - c_t^2 + \partial_y (c_l^2 - 2c_t^2)) \partial_y & c_t^2 k_x^2 + c_t^2 k_z^2 - c_t^2 \partial_y^2 - (\partial_y c_l^2) \partial_y & -ik_z (c_l^2 - c_t^2 + \partial_y (c_l^2 - 2c_t^2)) \partial_y \\ k_x k_z (c_l^2 - c_t^2) & -ik_z (c_l^2 - c_t^2 + \partial_y c_t^2) \partial_y & c_t^2 k_x^2 + c_t^2 k_z^2 - c_t^2 \partial_y^2 - (\partial_y c_t^2) \partial_y \end{pmatrix}. \quad (97)$$

The stress tensors become

$$\sigma_{xy} = \frac{\partial F}{\partial u_{xy}} = 2\rho c_t^2 u_{xy} \quad (98)$$

$$\sigma_{yz} = \frac{\partial F}{\partial u_{yz}} = 2\rho c_t^2 u_{yz} \quad (99)$$

$$\sigma_{yy} = \frac{\partial F}{\partial u_{yy}} = \rho c_l^2 u_{yy} + \rho (c_l^2 - 2c_t^2) (u_{xx} + u_{zz}) \quad (100)$$

The surface elastic wave solution of the isotropic model can be solved analytically (in the absence of the axion term), as presented in Refs. [41, 62]. We start out with the equation of motion in Eq. 96 and decompose the displacement field into the longitudinal and transverse components, $\mathbf{u}_t + \mathbf{u}_l$ $\mathbf{u} = \mathbf{u}_t + \mathbf{u}_l$, with $\nabla \cdot \mathbf{u}_t = 0$ and $\nabla \times \mathbf{u}_l = 0$. Since

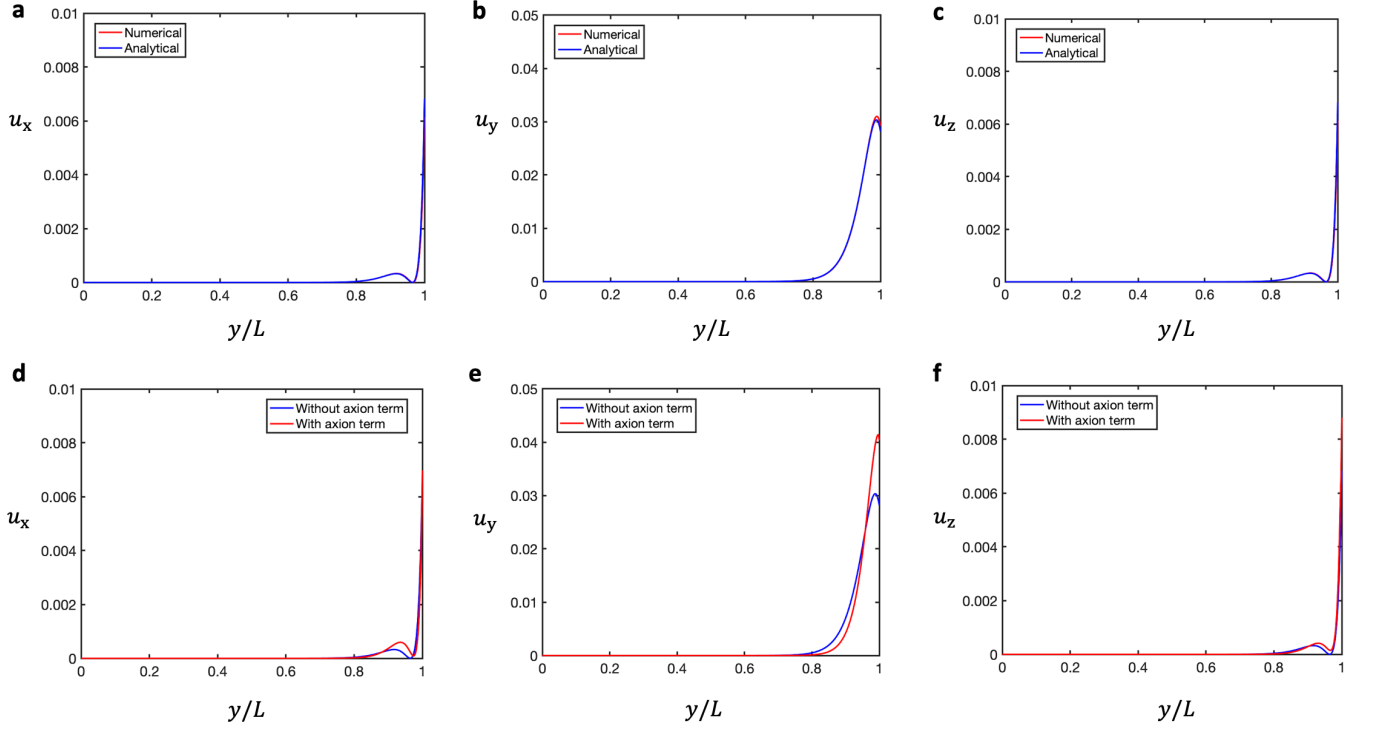


FIG. S9. (a) The components of the surface phonon mode displacement field are shown as (a) u_x (b) u_y (c) u_z in the absence of the axion term. In the presence of the axion term, the modified components of surface phonon mode displacement field are shown as (d) u_x (e) u_y (f) u_z . We use $r = .8$; $s = .713$; $t = .9$ in units of $10^{-12}m^4/s^2$. For both the plots we consider $k_x = k_z = 2.5nm^{-1}$ and the isotropic approximation with $c_t = 1.5$ and $c_l = 1.5$ in units of $10^6m^2/s^2$.

we consider a semi-infinite system, we expect a surface wave solution of the form $u_{t,i} = \alpha_i e^{ik_x x + ik_z z - i\omega t + \kappa_t y}$ and $u_{l,i} = \beta_i e^{ik_x x + ik_z z - i\omega t + \kappa_l y}$ with $\kappa_{t,l} = \sqrt{k^2 - \omega^2/c_{t,l}^2}$. The surface wave dispersion is of the form

$$\omega = \xi c_t k \quad (101)$$

with $k = \sqrt{k_x^2 + k_z^2}$, $\xi < 1$, which is determined from

$$\xi^6 - 8\xi^4 + 8(3 - 2c_t^2/c_l^2)\xi^2 - 16(1 - c_t^2/c_l^2) = 0. \quad (102)$$

The surface wave solution is

$$\mathbf{u} = N \begin{pmatrix} k_x \left[e^{\kappa_t y} - \frac{1}{2\kappa_t \kappa_l} (\kappa_t^2 + k^2) e^{\kappa_l y} \right] \\ -\frac{i}{\kappa_t} \left[k^2 e^{\kappa_t y} - (\kappa_t^2 + k^2) e^{\kappa_l y} \right] \\ k_z \left[e^{\kappa_t y} - \frac{1}{2\kappa_t \kappa_l} (\kappa_t^2 + k^2) e^{\kappa_l y} \right] \end{pmatrix} e^{ik_x x + ik_z z - i\omega t} \quad (103)$$

with the normalization factor N .

C. Numerical method

We follow the numerical calculation along the lines of Eqs(84,85) in the isotropic approximation with

$$\frac{\partial \theta}{\partial y}(y_n) = \begin{cases} -\theta_0/h, & \text{if } n = N + 1. \\ 0, & \text{otherwise.} \end{cases} \quad (104)$$

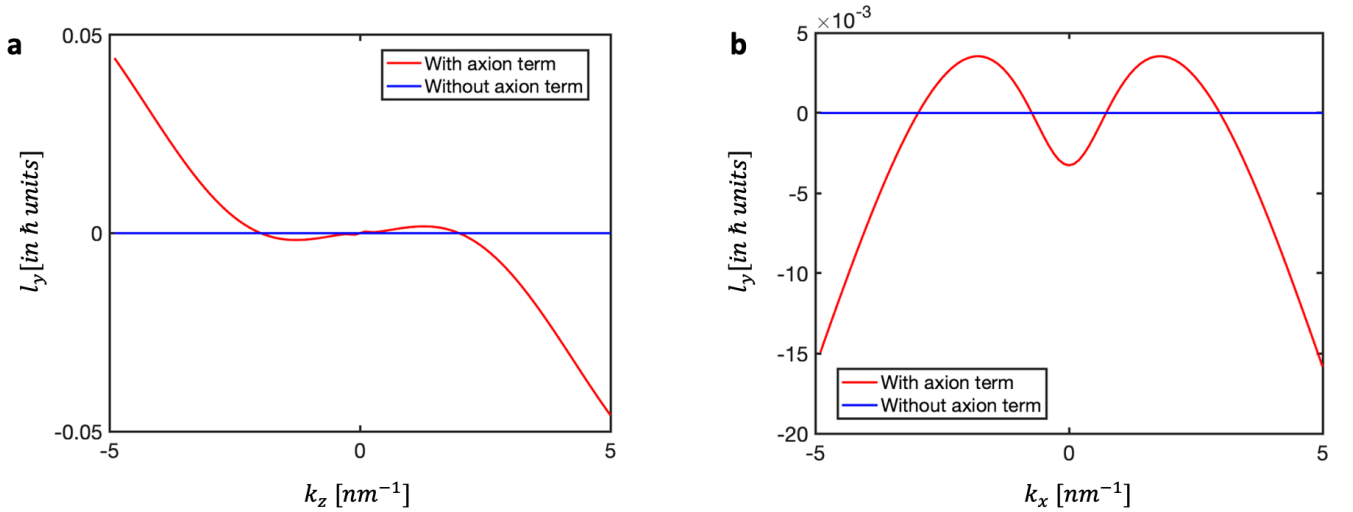


FIG. S10. (a) The out-of-plane (y -direction) angular momentum of the surface phonon mode l_y as a function of k_z along the $k_x = k_z$ line (b) The out-of-plane (y -direction) angular momentum of the surface phonon mode l_y as a function of k_x for $k_z = 1 \text{ nm}^{-1}$. For both the plots, we use $r = .8$; $s = .713$; $t = .9$ in units of $10^{-12} \text{ m}^4/\text{s}^2$ and the isotropic approximation with $c_t = 1.5$ and $c_l = 1.5$ in units of $10^6 \text{ m}^2/\text{s}^2$.

Stress free boundary conditions in Eqs(98-100) at site (boundary) $N + 1$ can be written generally as

$$\begin{aligned}
 \sigma_{iy}(y_{N+1}) = 0 &\implies \sum_{qt} \lambda_{iyqt} \partial_q u_l(y_{N+1}) = 0 \\
 \implies \sum_{q=x,z;l} ik_q \frac{\lambda_{iyql}(y_{N+1}) + \lambda_{lyqi}(y_{N+2})}{2} u_l(y_{N+1}) + \sum_l \frac{\lambda_{iyyl}(y_{N+2}) + \lambda_{lyyl}(y_{N+2})}{2} \frac{u_l(y_{N+2}) - u_l(y_{N+1})}{h} &= 0 \\
 \implies \sum_{q=x,z;l} -\frac{ik_q}{2h} [\lambda_{iyql}(y_{N+1}) + \lambda_{lyqi}(y_{N+2})] u_l(y_{N+1}) + \sum_l \frac{1}{2h^2} [\lambda_{iyyl}(y_{N+2}) + \lambda_{lyyl}(y_{N+1})] u_l(y_{N+1}) \\
 - \sum_l \frac{1}{2h^2} [\lambda_{iyyl}(y_{N+2}) + \lambda_{lyyl}(y_{N+1})] u_l(y_{N+2}) &= 0 \tag{105}
 \end{aligned}$$

Here, we choose $\lambda_{lyqi}(y_{N+2}) = \lambda_{iyql}(y_{N+1})$ and $\lambda_{iyyl}(y_{N+2}) = \lambda_{lyyl}(y_{N+2}) = \lambda_{iyyl}(y_{N+1})$. We make $\partial_q \rightarrow ik_q$ when $q = x, z$. Finally, we solve Eqs(84,85,104,105).

D. Numerical Results

In this section, we study the influence of the axion term on the surface acoustic phonon modes and the main numerical results are shown in Fig. S8-S10. In the absence of the axion term, from Sec.S4B, there exists a surface acoustic phonon mode with a linear frequency dispersion below the bulk bands, as shown in Fig. S8a, where the energy calculated numerically matches pretty well with the analytical expression (101) in Sec.S4B. The axion term further lowers the frequency of surface phonon modes, as shown in Fig. S8b. In the absence of the axion term, all the three components of the surface phonon displacement field \mathbf{u} are localized around the surface $y = L$ and exponentially decay away from the surface, as shown in Fig. S9(a-c). For these plots, along $k_x = k_z$, u_x and u_z follow the same decaying behavior, consistent with Eq.(103). In the presence of the axion term, all the three components of the surface phonon displacement field \mathbf{u} are further localized around the surface $y = L$, as shown in Fig. S9(d-f). Due to the anisotropy in the axion term, u_x and u_z follow different behaviors. The major qualitative change induced by the axion term is the appearance of a non-zero out-of-plane (y -direction) angular momentum (l_y) of the surface phonon mode, as demonstrated in Fig. S10a and b. We observe that $l_y(k_x, k_z) = -l_y(-k_x, -k_z)$, from Fig. S10a, in which we plot l_y along the $k_x = k_z$ line, and $l_y(k_x, k_z) = l_y(-k_x, k_z)$, from Fig. S10b, in which k_z is a fixed number. The former can be understood from time reversal \hat{T} , while the latter is a consequence of the combined effect of \hat{T} and z -directional mirror \hat{m}_z . The total phonon angular momentum, summed over all momenta k_x and k_z is zero. Therefore, in order

to probe the surface phonon mode via its angular momentum properties, a thermal gradient is required to bring the system away from equilibrium, which has been discussed in details in Sec. S5.

E. Hermiticity of the Hamiltonian

In this section, we discuss the hermiticity of our Hamiltonian. In particular, we show that for a free boundary condition, the continuum model Hamiltonians in Eqs(57,94) are hermitian.

1. Hermiticity of Eq(57)

Consider $\langle \mathbf{v} | H_0 | \mathbf{u} \rangle$ where H_0 is given by Eq(57), $\mathbf{u} = (u_x(y), u_y(y), u_z(y))^T$ and $\mathbf{v} = (v_x(y), v_y(y), v_z(y))^T$. Here, the domain of H_0 , $D(H_0) = \{ \mathbf{u} \in H^2(0, L) : u_x(0) = u_y(0) = u_z(0) = 0, \sigma_{xy}(L) = \sigma_{yz}(L) = \sigma_{yx}(L) = 0 \}$. The σ 's are given by Eqs(88-90).

$$\begin{aligned}
\langle \mathbf{v} | H_0 | \mathbf{u} \rangle &= \int_0^L dy v_x^* \left[((a+b)k_x^2 + dk_z^2 - \rho\omega^2 - b\partial_y^2) u_x - iak_x \partial_y u_y + (c+d)k_x k_z u_z \right] \\
&+ \int_0^L dy v_y^* \left[-iak_x \partial_y u_x + (bk_x^2 + dk_z^2 - \rho\omega^2 - (a+b)\partial_y^2) u_y - i(c+d)k_z \partial_y u_z \right] \\
&+ \int_0^L dy v_z^* \left[(c+d)k_x k_z u_x - i(c+d)k_z \partial_y u_y + (fk_z^2 + dk_x^2 - \rho\omega^2 - d\partial_y^2) u_z \right] \\
&= \overline{\langle \mathbf{u} | H_0^\dagger | \mathbf{v} \rangle} + \chi
\end{aligned} \tag{106}$$

with

$$\begin{aligned}
\chi &= -bv_x^* (\partial_y u_x) \Big|_0^L + b (\partial_y u_x^*) \Big|_0^L - iak_x v_x^* u_y \Big|_0^L - iak_x v_y^* u_x \Big|_0^L - (a+b)v_y^* (\partial_y u_y) \Big|_0^L + (a+b) (\partial_y v_y^*) u_y \Big|_0^L \\
&- i(c+d)k_z v_y^* u_z \Big|_0^L - i(c+d)k_z v_z^* u_y \Big|_0^L - dv_z^* (\partial_y u_z) \Big|_0^L + d (\partial_y v_z^*) u_z \Big|_0^L \\
&= -bv_x^*(L)u'_x(L) + bv_x^*(0)u'_x(0) + bv_x^*(L)u_x(L) - iak_x v_x^*(L)u_y(L) - iak_x v_y^*(L)u_x(L) \\
&- (a+b)v_y^*(L)u'_y(L) + (a+b)v_y^*(0)u'_y(0) + (a+b)v_y^*(L)u_y(L) - i(c+d)k_z v_y^*(L)u_z(L) \\
&- i(c+d)k_z v_z^*(L)u_y(L) - dv_z^*(L)u'_z(L) + dv_z^*(0)u'_z(0) + dv_z^*(L)u_z(L)
\end{aligned}$$

where we used open boundary conditions ($\mathbf{u}(0) = 0$). We also use the free boundary conditions (Eqs(88)-90) i.e.

$$\begin{aligned}
u'_x(L) + ik_x u_y(L) &= 0 \\
u'_z(L) + ik_z u_y(L) &= 0 \\
(a+b)u'_y(L) + (a-b)ik_x u_x(L) + cik_z u_z(L) &= 0
\end{aligned} \tag{107}$$

We have

$$\begin{aligned}
\chi &= ibk_x v_x^*(L)u_y(L) + bv_x^*(0)u'_x(0) + bv_x^*(L)u_x(L) - iak_x v_x^*(L)u_y(L) - iak_x v_y^*(L)u_x(L) \\
&+ i(a-b)k_x v_y^*(L)u_x(L) + ik_z c v_y^*(L)u_z(L) + (a+b)v_y^*(0)u'_y(0) + (a+b)v_y^*(L)u_y(L) \\
&- i(c+d)k_z v_y^*(L)u_z(L) - i(c+d)k_z v_z^*(L)u_y(L) + idk_z v_z^*(L)u_y(L) + dv_z^*(0)u'_z(0) + dv_z^*(L)u_z(L) \\
&= \left[(a+b)v_y^*(L) - i(a-b)k_x v_x^*(L) - ick_z v_z^*(L) \right] u_y(L) + b \left[v_x^*(L) - ik_x v_y^*(L) \right] u_x(L) \\
&+ d \left[v_z^*(L) - ik_z v_y^*(L) \right] u_z(L) + bv_x^*(0)u'_x(0) + (a+b)v_y^*(0)u'_y(0) + dv_z^*(0)u'_z(0)
\end{aligned} \tag{108}$$

For $\chi = 0$, we need \mathbf{v} to obey the same boundary conditions as \mathbf{u} . Therefore, $D(H_0) = D(H_0^\dagger)$ and H_0 is self-adjoint.

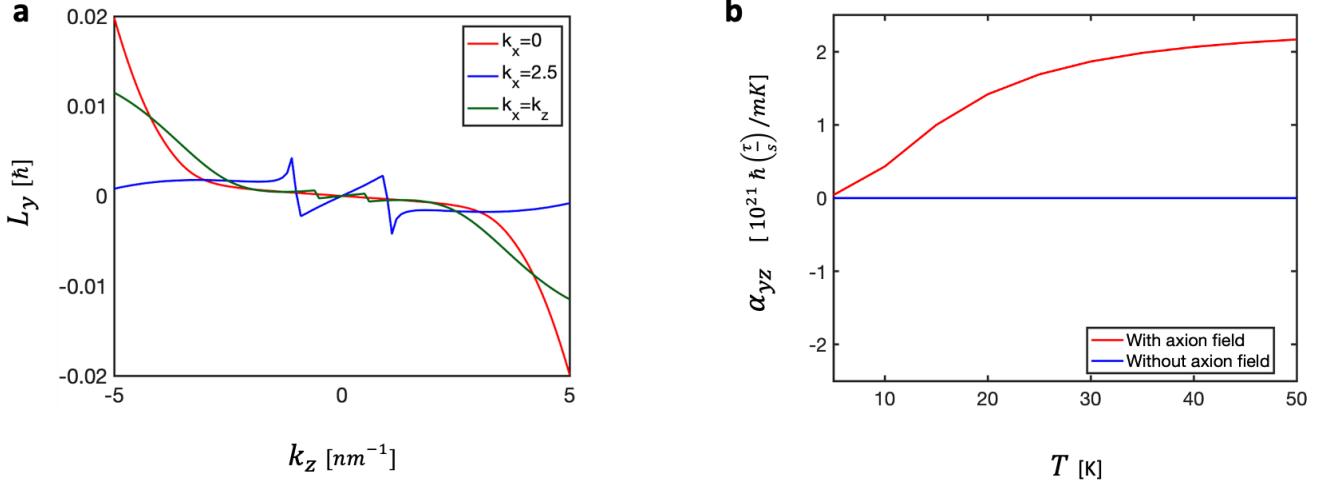


FIG. S11. (a) The out of plane (y direction) phonon angular momentum of the interface mode at $k_x = 0$ (red), $k_x = 2.5 \text{ nm}^{-1}$ (blue) and $k_x = k_z$ (dark green). (b) The y -direction angular momentum response to the z -direction thermal gradient, α_{yz} , of the interface phonon mode as a function of temperature in the presence (red) and absence (blue) of the axion field. We use $r = .8$; $s = .713$; $t = .9$ in units of $10^{-12} \text{ m}^4 / \text{s}^2$.

2. Hermiticity of Eq(94)

Consider $\langle \mathbf{v} | H_1 | \mathbf{u} \rangle$ where H_1 is given by Eq(94).

$$\begin{aligned}
 \langle \mathbf{v} | H_1 | \mathbf{u} \rangle &= -\langle \mathbf{v} | \frac{\partial \theta}{\partial y} h_1 | \mathbf{u} \rangle - \langle \mathbf{v} | \frac{\partial^2 \theta}{\partial y^2} h_2 | \mathbf{u} \rangle \\
 &= -\frac{\partial \theta}{\partial y} \langle \mathbf{v} | h_1 | \mathbf{u} \rangle - \langle \mathbf{v} | \frac{\partial \theta}{\partial y} \partial_y (h_2 | \mathbf{u} \rangle) \\
 &= -\frac{\partial \theta}{\partial y} \langle \mathbf{v} | h_1 | \mathbf{u} \rangle - \frac{\partial \theta}{\partial y} \langle \mathbf{v} | \partial_y (h_2 | \mathbf{u} \rangle)
 \end{aligned} \tag{109}$$

From Eq(94), we see that $h_1^\dagger = h_1$ and $h_2^\dagger = -h_2$, which makes h_1 hermitian and h_2 anti-hermitian. The first term $-\frac{\partial \theta}{\partial y} \langle \mathbf{v} | h_1 | \mathbf{u} \rangle$ is hermitian as $h_1^\dagger = h_1$. The second term $-\frac{\partial \theta}{\partial y} \langle \mathbf{v} | \partial_y (h_2 | \mathbf{u} \rangle)$ is also hermitian because it consists of the product of two anti-hermitian operators ∂_y and h_2 .

S5. ANGULAR MOMENTUM OF PHONON MODES

A. Derivation of total angular momentum for a lattice configuration

In this section, we outline the angular momentum calculation for phonon modes. This formalism can be applied to both the interfacial phonon mode at the axion domain wall (presented in the main text) as well as the surface phonon mode described in Sec. S4. Phonon angular momentum has been previously described in Refs. [52, 53]. We consider a lattice model along the y direction, where k_x and k_z are good quantum numbers, but k_y is not a good quantum number due to the domain wall structure. We write the mode expansion for the displacement field and the corresponding canonical momentum in terms of the a and a^\dagger as

$$u_i(x, y, z) = \int \frac{dk_x}{(2\pi)} \frac{dk_z}{(2\pi)} \sum_{\alpha, n} \sqrt{\frac{\hbar}{2\rho\omega_n^\alpha(k_x, k_z)}} \epsilon_i^\alpha(k_x, k_z, y, n) \left[a_n^\alpha(k_x, k_z) e^{i(k_x x + k_z z - \omega_n^\alpha(k_x, k_z)t)} \right] + h.c \tag{110}$$

$$\Pi_i(x, y, z) = -i \int \frac{dk_x}{(2\pi)} \frac{dk_z}{(2\pi)} \sum_{\alpha, n} \sqrt{\frac{\hbar\rho\omega_n^\alpha(k_x, k_z)}{2}} \epsilon_i^\alpha(k_x, k_z, y, n) \left[a_n^\alpha(k_x, k_z) e^{i(k_x x + k_z z - \omega_n^\alpha(k_x, k_z)t)} \right] + h.c \tag{111}$$

where the index α in ϵ^α labels $\alpha = 1, 2, 3$ which represent 3 possible polarizations. In the isotropic limit, these correspond to 1 longitudinal polarization and 2 transverse polarizations. n labels the quantum number corresponding to the y -direction confinement, i.e. $n = 1, 2, \dots, N+1$, for $N+1$ quantum well states. The operator $a_n^\alpha(k_x, k_z)$ creates a phonon described by the eigenvector $\vec{e}^\alpha(k_x, k_z, y, n)$ with polarization α , the quantum number n , momenta k_x and k_z . ω_n^α labels the eigen frequency. We now define $\vec{r} = x\hat{e}_x + z\hat{e}_z$ and $\vec{k} = k_x\hat{e}_x + k_z\hat{e}_z$. The angular momentum $j_i(x, y, z)$ is given by

$$\begin{aligned} j_i(x, y, z) &= \epsilon_{ijl} u_j(x, y, z) \Pi_l(x, y, z) \\ &= -i\epsilon_{ijl} \frac{\hbar}{2} \sum_{\alpha, \beta, n, m} \int \frac{d^2k}{(2\pi)^2} \frac{d^2k'}{(2\pi)^2} \sqrt{\frac{\omega_m^\beta(\vec{k})}{\omega_n^\alpha(\vec{k}')}} \left[\epsilon_j^\alpha(\vec{k}, y, n) a_n^\alpha(\vec{k}) e^{i(\vec{k} \cdot \vec{r} - \omega_n^\alpha(\vec{k})t)} + \epsilon_j^\alpha(\vec{k}, y, n)^* a_n^\alpha(\vec{k})^\dagger e^{-i(\vec{k} \cdot \vec{r} - \omega_n^\alpha(\vec{k})t)} \right] \\ &\times \left[\epsilon_j^\beta(\vec{k}', y, m) a_m^\beta(\vec{k}') e^{i(\vec{k}' \cdot \vec{r} - \omega_m^\beta(\vec{k}')t)} - \epsilon_j^\beta(\vec{k}', y, m)^* a_m^\beta(\vec{k}')^\dagger e^{-i(\vec{k}' \cdot \vec{r} - \omega_m^\beta(\vec{k}')t)} \right]. \end{aligned} \quad (112)$$

The total angular momentum is defined as $J_i = \sum_y \int d^2r j_i(x, y, z)$. We integrate Eq(112) over the xz surface and sum over all y sites. We make use of the relation $\int d^2r e^{i(\vec{k} - \vec{k}') \cdot \vec{r}} = (2\pi)^2 \delta^2(\vec{k} - \vec{k}')$ and find

$$\begin{aligned} J_i &= -i\epsilon_{ijl} \frac{\hbar}{2} \sum_{\alpha, \beta, n, m, y} \int \frac{d^2k}{(2\pi)^2} \sqrt{\frac{\omega_m^\beta(\vec{k})}{\omega_n^\alpha(\vec{k})}} \left[\epsilon_j^\alpha(\vec{k}, y, n)^* \epsilon_l^\beta(\vec{k}, y, m) a_n^\alpha(\vec{k})^\dagger a_m^\beta(\vec{k}) e^{i(\omega_n^\alpha(\vec{k}) - \omega_m^\beta(\vec{k}))t} \right. \\ &\quad \left. - \epsilon_j^\alpha(\vec{k}, y, n) \epsilon_l^\beta(\vec{k}, y, m)^* a_n^\alpha(\vec{k}) a_m^\beta(\vec{k})^\dagger e^{-i(\omega_n^\alpha(\vec{k}) - \omega_m^\beta(\vec{k}))t} \right]. \end{aligned} \quad (113)$$

Since the system is in equilibrium, we have neglected terms of the form aa and $a^\dagger a^\dagger$. Furthermore, for the second term on the right side of Eq(113), we can switch the indices j and l and write $-\epsilon_{ijl} \epsilon_j^\alpha(n) (\epsilon_l^\beta(m))^* = \epsilon_{ijl} \epsilon_l^\alpha(n) \epsilon_j^\beta(m)^*$. We define $(M_i)_{jl} = -i\hbar \epsilon_{ijl}$ and find

$$\begin{aligned} J_i &= \frac{1}{2} \sum_{\alpha, \beta, m, n, y} \int \frac{d^2k}{(2\pi)^2} \sqrt{\frac{\omega_m^\beta(\vec{k})}{\omega_n^\alpha(\vec{k})}} \epsilon_j^\alpha(\vec{k}, y, n)^* (M_i)_{jl} \epsilon_l^\beta(\vec{k}, y, m) \left[a_n^\alpha(\vec{k})^\dagger a_m^\beta(\vec{k}) e^{i(\omega_n^\alpha(\vec{k}) - \omega_m^\beta(\vec{k}))t} \right. \\ &\quad \left. + a_n^\alpha(\vec{k}) a_m^\beta(\vec{k})^\dagger e^{-i(\omega_n^\alpha(\vec{k}) - \omega_m^\beta(\vec{k}))t} \right]. \end{aligned} \quad (114)$$

We use the commutation relation $[a_n^\alpha(\vec{k}), a_m^\beta(\vec{k}')^\dagger] = (2\pi)^2 \delta^2(\vec{k} - \vec{k}') \delta_{\alpha, \beta} \delta_{n, m}$. In equilibrium, $\langle a_n^\alpha(\vec{k})^\dagger a_m^\beta(\vec{k}) \rangle_0 = f(\omega_n^\alpha(\vec{k})) \delta_{\alpha, \beta} \delta_{n, m}$, where $f(\omega_n^\alpha(\vec{k}))$ is the Bose distribution. Therefore, the total angular momentum is given by

$$J_i = \int \frac{d^2k}{(2\pi)^2} \sum_{\alpha, n, y} l_i^\alpha(\vec{k}, y, n) \left[f(\omega_n^\alpha(\vec{k})) + 1/2 \right], \quad l_i^\alpha(\vec{k}, y, n) = \epsilon_j^\alpha(\vec{k}, y, n)^* (M_i)_{jl} \epsilon_l^\alpha(\vec{k}, y, n). \quad (115)$$

B. Effect of thermal gradient

We now consider the system away from equilibrium. In order to invoke Boltzman transport theory [53, 63], we assume small deviation away from equilibrium. We also assume that the phonon relaxation process quickly brings the system back to thermal equilibrium, which can be characterized by the relaxation time τ . In this semiclassical picture, both \vec{k} and \vec{r} are well-defined and we consider the phase space (x, z, k_x, k_z) . The distribution function $f^\alpha(\vec{r}, \vec{k}, n, t)$ is the probability of an electron at \vec{r} occupying the state \vec{k} with n and α at time t . The equilibrium state of phonons satisfies the Bose-Einstein distribution. In the absence of collisions, we have for a particular n and α ,

$$\vec{r}(t - dt) = \vec{r}(t) - \vec{v}_n^\alpha(\vec{k}) dt, \quad (116)$$

$$\vec{k}(t - dt) = \vec{k}(t) - \frac{1}{\hbar} \vec{F}(\vec{r}, \vec{k}, t) dt, \quad (117)$$

where $\vec{v}_n^\alpha(\vec{k})$ is the group velocity given by $\vec{v}_n^\alpha(\vec{k}) = \frac{1}{\hbar} \frac{\partial E_n^\alpha(\vec{k})}{\partial \vec{k}} = \frac{1}{\hbar} \frac{\partial}{\partial \vec{k}} \left(\rho \omega_n^\alpha(\vec{k})^2 \right)$. For the next few lines of the derivation, we omit the indices n and α but bring them back at the end of the derivation. Liouville's theorem requires

$$\begin{aligned} f(\vec{r}, \vec{k}, t) &= f\left(\vec{r} - \vec{v}(\vec{k})dt, y, \vec{k} - dt\right) \\ &= f(\vec{r}, \vec{k}, t) - \left(\vec{\nabla}_r f\right) \cdot \vec{v}(\vec{k})dt - \frac{\partial f}{\partial t} dt \end{aligned} \quad (118)$$

Rearranging the terms, we have

$$\frac{\partial f}{\partial t} + \vec{v} \cdot \left(\vec{\nabla}_r f\right) = 0 \quad (119)$$

We add the collision term $\left(\frac{\partial f}{\partial t}\right)_{\text{coll}}$ to the right-hand side of the above equation to take into account the relaxation process. In the relaxation-time approximation, the phenomenological ansatz is

$$\left(\frac{\partial f}{\partial t}\right)_{\text{coll}} = -\frac{1}{\tau} \left(f(\vec{r}, \vec{k}, t) - f_{\vec{k}}^0\right), \quad (120)$$

where τ is the relaxation time and $f_{\vec{k}}^0$ is the equilibrium distribution. Therefore, we have

$$\vec{v}(\vec{k}) \cdot \vec{\nabla}_r f = \left(\frac{\partial f}{\partial t}\right)_{\text{coll}} = -\frac{1}{\tau} \left(f(\vec{r}, \vec{k}, t) - f_{\vec{k}}^0\right) \quad (121)$$

We restore the indices n and α , so

$$\begin{aligned} f\left(\omega_n^\alpha(\vec{k})\right) &= f^0\left(\omega_n^\alpha(\vec{k})\right) - \tau \vec{v}_n^\alpha(\vec{k}) \cdot \vec{\nabla}_r f^0\left(\omega_n^\alpha(\vec{k})\right) \\ &= f^0\left(\omega_n^\alpha(\vec{k})\right) - \tau v_{i,n}^\alpha(\vec{k}) \frac{\partial f^0}{\partial T} \frac{\partial T}{\partial x_i}. \end{aligned} \quad (122)$$

Plugging Eq(122) into Eq(115), we have

$$J_i = \int \frac{d^2 k}{(2\pi)^2} \sum_{\alpha, y, n} l_i^\alpha(\vec{k}, y, n) \left[f\left(\omega_n^\alpha(\vec{k})\right) + 1/2 \right] = -\tau \int \frac{d^2 k}{(2\pi)^2} \sum_{\alpha, y, n} l_i^\alpha(\vec{k}, y, n) v_{j,n}^\alpha(\vec{k}) \frac{\partial f^0}{\partial T} \frac{\partial T}{\partial x_j}, \quad (123)$$

where we have used the fact that for a time reversal invariant system, $l^\alpha(-\vec{k}, y, n) = -l^\alpha(\vec{k}, y, n)$ but $f^0\left(\omega_n^\alpha(-\vec{k})\right) = f^0\left(\omega_n^\alpha(\vec{k})\right)$ i.e.

$$\int \frac{d^2 k}{(2\pi)^2} l_i^\alpha(\vec{k}, y, n) = 0 \quad (124)$$

$$\int \frac{d^2 k}{(2\pi)^2} l_i^\alpha(\vec{k}, y, n) f^0\left(\omega_n^\alpha(\vec{k})\right) = 0 \quad (125)$$

We rewrite Eq(123) as $J_i = \alpha_{ij} \frac{\partial T}{\partial x_j}$ and the response tensor is given by

$$\alpha_{ij} = -\tau \int \frac{d^2 k}{(2\pi)^2} \sum_{\alpha, y, n} l_i^\alpha(\vec{k}, y, n) v_{j,n}^\alpha(\vec{k}) \frac{\partial f^0}{\partial T} = -\frac{\tau}{A_{xz}} \sum_{\vec{k}, \alpha, y, n} l_i^\alpha(\vec{k}, y, n) v_{j,\alpha,n}^\alpha(\vec{k}) \frac{\partial f^0}{\partial T} \quad (126)$$

C. Symmetry properties of the response tensor α_{ij}

In order to probe the angular momentum response of the interfacial or surface phonon modes, the thermal gradient must be applied along the plane perpendicular to the axion domain wall i.e. along the xz plane. The response function forms a 3×2 matrix as the temperature gradient is restricted to the film plane. In the absence of the axion term, the symmetries of the xz plane are generated by $m_x : x \rightarrow -x$ and $m_z : z \rightarrow -z$. The axial tensor must obey $m_x \alpha m_x^{-1} = -\alpha$ and $m_z \alpha m_z^{-1} = -\alpha$. So

$$\alpha = \begin{pmatrix} 0 & \alpha_{xz} \\ 0 & 0 \\ \alpha_{zx} & 0 \end{pmatrix} \quad (127)$$

The axion surface term F_1 breaks m_x , therefore, $\alpha_{zy}, \alpha_{yz} \neq 0$. In the presence of the axion term

$$\alpha = \begin{pmatrix} 0 & \alpha_{xz} \\ 0 & \alpha_{yz} \\ \alpha_{zx} & 0 \end{pmatrix}, \quad (128)$$

which provides an additional α_{yz} term due to strain (axion term is created by strain) corresponding to the y -direction phonon angular momentum response due to the z -direction thermal gradient of the interfacial phonon mode. The phonon angular momentum in the momentum space is shown in Fig. S11a and the thermal gradient induced phonon angular momentum as a function of temperature is shown in Fig. S11b, in which the axion term is found to be essential for the component α_{yz} . α_{yz} is calculated to be $\sim 10^{21} \hbar \left(\frac{\tau}{s}\right) m^{-1} K^{-1} \sim 10^{-13} \left(\frac{\tau}{s}\right) Jsm^{-1} K^{-1}$. It should be noted that the total angular momentum defined in Eq.(115) is for a two dimensional slab, instead of a three dimensional (3D) bulk, so the unit of the coefficient α_{yz} is different from that defined in Ref.[53, 55]. For a comparison with the value of α for 3D bulk, we choose the decaying length l_d of the interfacial modes around $10 \sim 100\text{nm}$ as the inverse of decaying length $\lambda = 1/l_d$ is around $0.01 \sim 0.1\text{nm}^{-1}$. Using this length scale for the y direction, we can estimate $\alpha_{yz}/l_d \approx 10^{-6} \sim 10^{-5} \left(\frac{\tau}{s}\right) Jsm^{-2} K^{-1}$, which is comparable to the values of $\alpha \sim 10^{-6} \left(\frac{\tau}{s}\right) Jsm^{-2} K^{-1}$ from the previous studies of temperature gradient induced phonon angular momentum in bulk materials [53, 55].

-
- [1] X.-L. Qi and S.-C. Zhang, *Reviews of Modern Physics* **83**, 1057 (2011).
 - [2] M. Z. Hasan and C. L. Kane, *Reviews of modern physics* **82**, 3045 (2010).
 - [3] B. Yan and S.-C. Zhang, *Reports on Progress in Physics* **75**, 096501 (2012).
 - [4] B. J. Wieder, B. Bradlyn, J. Cano, Z. Wang, M. G. Vergniory, L. Elcoro, A. A. Soluyanov, C. Felser, T. Neupert, N. Regnault, *et al.*, *Nature Reviews Materials* **7**, 196 (2022).
 - [5] S. Ryu and Y. Hatsugai, *Physical review letters* **89**, 077002 (2002).
 - [6] A. P. Schnyder, S. Ryu, A. Furusaki, and A. W. Ludwig, *Physical Review B* **78**, 195125 (2008).
 - [7] R. S. Mong and V. Shivamoggi, *Physical Review B* **83**, 125109 (2011).
 - [8] S. Ryu, A. P. Schnyder, A. Furusaki, and A. W. Ludwig, *New Journal of Physics* **12**, 065010 (2010).
 - [9] Y. Tanaka, M. Sato, and N. Nagaosa, *Journal of the Physical Society of Japan* **81**, 011013 (2011).
 - [10] A. Kitaev, in *AIP conference proceedings*, Vol. 1134 (American Institute of Physics, 2009) pp. 22–30.
 - [11] Y. Hatsugai, *Solid state communications* **149**, 1061 (2009).
 - [12] L. Lu, J. D. Joannopoulos, and M. Soljačić, *Nature photonics* **8**, 821 (2014).
 - [13] T. Ozawa, H. M. Price, A. Amo, N. Goldman, M. Hafezi, L. Lu, M. C. Rechtsman, D. Schuster, J. Simon, O. Zilberberg, *et al.*, *Reviews of Modern Physics* **91**, 015006 (2019).
 - [14] Y. Liu, X. Chen, and Y. Xu, *Advanced Functional Materials* **30**, 1904784 (2020).
 - [15] H. Chen, W. Zhang, Q. Niu, and L. Zhang, *2D Materials* **6**, 012002 (2018).
 - [16] X.-Q. Chen, J. Liu, and J. Li, *The Innovation* **2** (2021).
 - [17] F. Zhuo, J. Kang, A. Manchon, and Z. Cheng, *Advanced Physics Research* , 2300054 (2023).
 - [18] P. A. McClarty, *Annual Review of Condensed Matter Physics* **13**, 171 (2022).
 - [19] E. J. Bergholtz, J. C. Budich, and F. K. Kunst, *Reviews of Modern Physics* **93**, 015005 (2021).
 - [20] M. J. Gilbert, *Communications Physics* **4**, 70 (2021).
 - [21] S. Zheng, G. Duan, and B. Xia, *Applied Sciences* **12**, 1987 (2022).
 - [22] G. Ma, M. Xiao, and C. T. Chan, *Nature Reviews Physics* **1**, 281 (2019).
 - [23] X. Mao and T. C. Lubensky, *Annual Review of Condensed Matter Physics* **9**, 413 (2018).

- [24] P. Thalmeier, *Physical Review B* **83**, 125314 (2011).
- [25] S. Giraud and R. Egger, *Physical Review B* **83**, 245322 (2011).
- [26] S. Giraud, A. Kundu, and R. Egger, *Physical Review B* **85**, 035441 (2012).
- [27] G. Huang, *Europhysics Letters* **100**, 17001 (2012).
- [28] V. Parente, A. Tagliacozzo, F. Von Oppen, and F. Guinea, *Physical Review B* **88**, 075432 (2013).
- [29] I. Garate, *Physical Review Letters* **110**, 046402 (2013).
- [30] T. Karzig, C.-E. Bardyn, N. H. Lindner, and G. Refael, *Physical Review X* **5**, 031001 (2015).
- [31] W. Liu, Z. Ji, Y. Wang, G. Modi, M. Hwang, B. Zheng, V. J. Sorger, A. Pan, and R. Agarwal, *Science* **370**, 600 (2020).
- [32] S. Klembt, T. Harder, O. Egorov, K. Winkler, R. Ge, M. Bandres, M. Emmerling, L. Worschech, T. Liew, M. Segev, *et al.*, *Nature* **562**, 552 (2018).
- [33] G. Hu, Q. Ou, G. Si, Y. Wu, J. Wu, Z. Dai, A. Krasnok, Y. Mazor, Q. Zhang, Q. Bao, *et al.*, *Nature* **582**, 209 (2020).
- [34] M. Li, I. Sinev, F. Benimetskiy, T. Ivanova, E. Khestanova, S. Kiriushchikina, A. Vakulenko, S. Guddala, M. Skolnick, V. M. Menon, *et al.*, *Nature communications* **12**, 4425 (2021).
- [35] Y. V. Kartashov and D. V. Skryabin, *Physical review letters* **122**, 083902 (2019).
- [36] Z. Liu, B. Zhou, Y. Zhang, Z. Wang, H. Weng, D. Prabhakaran, S.-K. Mo, Z. Shen, Z. Fang, X. Dai, *et al.*, *Science* **343**, 864 (2014).
- [37] J. Xiong, S. K. Kushwaha, T. Liang, J. W. Krizan, M. Hirschberger, W. Wang, R. J. Cava, and N. P. Ong, *Science* **350**, 413 (2015).
- [38] Z. Wang, Y. Sun, X.-Q. Chen, C. Franchini, G. Xu, H. Weng, X. Dai, and Z. Fang, *Physical Review B* **85**, 195320 (2012).
- [39] Z. Wang, H. Weng, Q. Wu, X. Dai, and Z. Fang, *Physical Review B* **88**, 125427 (2013).
- [40] See Supplementary Material at [URL]. In Sec. S1, we present the effective theory of Na_3Bi based on the symmetry properties of D_{6h} symmetry group with relevant material parameters. We derive the effective action S_{eff} and discuss the symmetry properties of S_{eff} . We close Sec. S1 with the bulk action and deriving the equation of motion in the presence of the axion term. In Sec. S2, we provide details of the analytical solutions for *Case I* and *Case II*. In Sec. S3, we provide the framework for our numerical calculations and elaborate on some of the numerical features presented in the main text. In Sec. S4, we perform detailed calculations to show the influence of the axion term on the already present surface modes of an elastic material with an open boundary. Lastly, in Sec. S5, we present the formalism for the phonon angular momentum and describe probing the helical nature of the interface phonon modes using a temperature gradient.
- [41] L. D. Landau, E. M. Lifshitz, A. M. Kosevich, and L. P. Pitaevskii, *Theory of elasticity: volume 7*, Vol. 7 (Elsevier, 1986).
- [42] F. de Juan, J. L. Manes, and M. A. Vozmediano, *Physical Review B* **87**, 165131 (2013).
- [43] D. Pikulin, A. Chen, and M. Franz, *Physical Review X* **6**, 041021 (2016).
- [44] R. Ilan, A. G. Grushin, and D. I. Pikulin, *Nature Reviews Physics* **2**, 29 (2020).
- [45] J. Yu and C.-X. Liu, in *Semiconductors and Semimetals*, Vol. 108 (Elsevier, 2021) pp. 195–224.
- [46] J. Yu, B. J. Wieder, and C.-X. Liu, *Physical Review B* **104**, 174406 (2021).
- [47] F. Wilczek, *Physical review letters* **58**, 1799 (1987).
- [48] A. Sekine and K. Nomura, *Journal of Applied Physics* **129** (2021).
- [49] D. M. Neno, C. A. Garcia, J. Gooth, C. Felser, and P. Narang, *Nature Reviews Physics* **2**, 682 (2020).
- [50] M. De Jong, W. Chen, T. Angsten, A. Jain, R. Notestine, A. Gamst, M. Sluiter, C. Krishna Ande, S. Van Der Zwaag, J. J. Plata, *et al.*, *Scientific data* **2**, 1 (2015).
- [51] X.-X. Dong, J.-X. Chen, Y. Wang, Z.-L. Lv, and H.-Y. Wang, *Materials Research Express* **6**, 076308 (2019).
- [52] L. Zhang and Q. Niu, *Physical Review Letters* **112**, 085503 (2014).
- [53] M. Hamada, E. Minamitani, M. Hirayama, and S. Murakami, *Physical review letters* **121**, 175301 (2018).
- [54] L.-H. Hu, J. Yu, I. Garate, and C.-X. Liu, *Physical review letters* **127**, 125901 (2021).
- [55] C.-X. Liu, *Physical Review B* **106**, 115102 (2022).
- [56] Z. Cheng, R. Li, X. Yan, G. Jernigan, J. Shi, M. E. Liao, N. J. Hines, C. A. Gadre, J. C. Idrobo, E. Lee, *et al.*, *Nature communications* **12**, 6901 (2021).
- [57] R. Qi, R. Shi, Y. Li, Y. Sun, M. Wu, N. Li, J. Du, K. Liu, C. Chen, J. Chen, *et al.*, *Nature* **599**, 399 (2021).
- [58] M. M. Otrokov, I. I. Klimovskikh, H. Bentmann, D. Estyunin, A. Zeugner, Z. S. Aliev, S. Gaß, A. Wolter, A. Koroleva, A. M. Shikin, *et al.*, *Nature* **576**, 416 (2019).
- [59] D. Zhang, M. Shi, T. Zhu, D. Xing, H. Zhang, and J. Wang, *Physical review letters* **122**, 206401 (2019).
- [60] J. Li, Y. Li, S. Du, Z. Wang, B.-L. Gu, S.-C. Zhang, K. He, W. Duan, and Y. Xu, *Science Advances* **5**, eaaw5685 (2019).
- [61] R. Winkler, S. Papadakis, E. De Poortere, and M. Shayegan, *Spin-orbit coupling in two-dimensional electron and hole systems*, Vol. 41 (Springer, 2003).
- [62] W. Kress and F. W. de Wette, *Surface phonons* (Springer, 1991).
- [63] S. M. Girvin and K. Yang, *Modern condensed matter physics* (Cambridge University Press, 2019).